Materials Today Bio 24 (2024) 100937

Contents lists available at ScienceDirect

Materials Today Bio

journal homepage: www.journals.elsevier.com/materials-today-bio

A basement membrane extract-based three-dimensional culture system promotes the neuronal differentiation of cochlear Sox10-positive glial cells *in vitro*

Junze Lu [a,b,1], Man Wang [a,b,1], Xue Wang [a,b], Yu Meng [a,b], Fang Chen [a,b], Jinzhu Zhuang [a,b], Yuechen Han [a,b], Haibo Wang [a,b,**], Wenwen Liu [a,b,*]

[a] Department of Otolaryngology-Head and Neck Surgery, Shandong Provincial ENT Hospital, Shandong University, Jinan, 250022, China
[b] Shandong Institute of Otorhinolaryngology, Jinan, 250022, China

ARTICLE INFO

Keywords:
Hearing loss
Spiral ganglion neuron
Glial cell
Differentiation
Basement membrane extract-based three-dimensional culture
Sox10

ABSTRACT

Spiral ganglion neurons (SGNs) in the mammalian cochleae are essential for the delivery of acoustic information, and damage to SGNs can lead to permanent sensorineural hearing loss as SGNs are not capable of regeneration. Cochlear glial cells (GCs) might be a potential source for SGN regeneration, but the neuronal differentiation ability of GCs is limited and its properties are not clear yet. Here, we characterized the cochlear Sox10-positive (Sox10+) GCs as a neural progenitor population and developed a basement membrane extract-based three-dimensional (BME-3D) culture system to promote its neuronal generation capacity *in vitro*. Firstly, the purified Sox10+ GCs, isolated from Sox10-creER/tdTomato mice via flow cytometry, were able to form neurospheres after being cultured in the traditional suspension culture system, while significantly more neurospheres were found and the expression of stem cell-related genes was upregulated in the BME-3D culture group. Next, the BME-3D culture system promoted the neuronal differentiation ability of Sox10+ GCs, as evidenced by the increased number, neurite outgrowth, area of growth cones, and synapse density as well as the promoted excitability of newly induced neurons. Notably, the BME-3D culture system also intensified the reinnervation of newly generated neurons with HCs and protected the neurospheres and derived-neurons against cisplatin-induced damage. Finally, transcriptome sequencing analysis was performed to identify the characteristics of the differentiated neurons. These findings suggest that the BME-3D culture system considerably promotes the proliferation capacity and neuronal differentiation efficiency of Sox10+ GCs *in vitro*, thus providing a possible strategy for the SGN regeneration study.

1. Introduction

Spiral ganglion neurons (SGNs) in the mammalian inner ear are the first neural element in the auditory conduction pathway, as they acquire and deliver acoustic information from cochlear hair cells (HCs) to the central nervous system, thereby allowing the establishment of auditory cognition [1]. As terminally differentiated cells, SGNs cannot regenerate by themselves, and thus any damage to them due to genetic or environmental factors leads to irreversible sensorineural hearing loss (SNHL) [2]. However, currently, there is no effective treatment to biologically replace damaged SGNs. Recent studies revealed the existence of stem cells in the postnatal inner ear [3–6], among these potential stem cells, isolated cells from the spiral ganglion, which contains cochlear glial cells (GCs), are able to form spherical structures and differentiate into

Abbreviations: 3D, three-dimensional; BME, basement membrane extract; CCK8, Cell Counting Kit-8; DIV, day *in vitro*; DM, differentiation medium; ECM, extracellular matrix; EdU, 5-ethynyl-2′-deoxyuridine; FACS, fluorescence-activated cell sorting; FM, full medium; GCs, glial cells; HCs, hair cells; NCCs, neural crest cells; NSPs, neural stem/progenitor cells; LNL, longest neurite length; OC, organ of Corti; PBS, phosphate-buffered saline; PCR, polymerase chain reaction; PFA, paraformaldehyde; RT-PCR, real-time PCR; SGNs, spiral ganglion neurons; SNHL, sensorineural hearing loss; Sox10, SRY-box transcription factor 10; TUNEL, terminal deoxynucleotidyl transferase dUTP nick end labeling; AP, action potential.

* Corresponding author. Department of Otolaryngology-Head and Neck Surgery, Shandong Provincial ENT Hospital, Shandong University, Jinan, 250022, China.
** Corresponding author. Department of Otolaryngology-Head and Neck Surgery, Shandong Provincial ENT Hospital, Shandong University, Jinan, 250022, China.
E-mail addresses: whboto11@email.sdu.edu.cn (H. Wang), wenwenliu@email.sdu.edu.cn (W. Liu).
[1] Junze Lu and Man Wang contributed equally to this work.

https://doi.org/10.1016/j.mtbio.2023.100937
Received 11 October 2023; Received in revised form 14 December 2023; Accepted 27 December 2023
Available online 28 December 2023

SGNs-like cells [7]. In the mammalian embryo, both inner ear SGNs and GCs are derived from the ectoderm [8], the otic placode invaginates to form the otic vesicle and further develop into the SGNs, whereas neural crest cells (NCCs) that delaminate from the dorsal neural tube give rise to GCs [8,9]. In the postnatal cochlea, GCs are involved in promoting the development and survival of SGNs by providing neuregulin and neurotrophic support [10–12], as well as maintaining the proper function of SGN [13]. Recently, studies have identified the neonatal inner ear GCs as a potential source of neural stem/progenitor cells (NSPs) for SGN regeneration [2]. For example, the quiescent GCs could be activated and initiate proliferation after SGN degeneration [7,14], several subtypes of GCs, such as proteolipid protein (PLP1)-positive GCs [4], Sox2-positive glial population [15], can give rise to neurons and GCs, but not HCs, *in vitro* or *in vivo*. SGN regeneration from in situ cochlear GCs has many advantages [2] such as technical ease of implementation without the need for exogenous cell transplantation and a reduced risk of tumor formation [16]. However, the numbers of these reported GCs as well as their neuronal differentiation capacity are quite limited, therefore, strategies to promote the proliferation, neuronal differentiation, and survival of inner ear NSPs will be conducive to developing strategies for SGN regeneration and hearing restoration.

SRY-box transcription factor 10 (Sox10), a transcription factor belonging to the SoxE family which is known to regulate embryonic processes and determine the cell fate in various tissues [17], is expressed in NCCs and specifically regulates NCCs into GCs in the cochleovestibular ganglion (CVG) [18,19]. The deficiency of the Sox10 gene induces a shortened cochlear duct and defect of GCs in the embryo, although the formation of HCs in the organ of Corti and the neuronal differentiation in the CVG are normal [9,18]. These features indicate that Sox10 is indispensable for the development of the inner ear, especially for GC formation and development. However, the properties of cochlear Sox10 positive (Sox10+) GCs and their potential for neuronal differentiation have not been explored.

The use of three-dimensional (3D) culture system is increasingly prevalent in optimizing *in vitro* stem cell cultures. This system is more closely resemble the natural cellular environment, fostering enhanced interactions between cells and their surrounding matrix. This environment is crucial in maintaining or enhancing specific cellular traits, offering a significant advantage over traditional two-dimensional (2D) culture system. In the context of auditory research, biomaterial-based 3D cultures have shown promise in aiding the regeneration of cochlear cells, including HCs [20] and SGNs [21] from externally sourced stem cells. Various biomaterials, including hydrogel [22], polymers [23], and other porous scaffolds materials [24], are utilized to construct these 3D cultures. The basement membrane extract (BME), a soluble form of extracellular matrix (ECM) purified from developing embryo or tumor tissues, could be cross-linked at 37 °C to form hydrogel [25] and has excellent biocompatibility, bioactivity, and tunable mechanical properties [26]. Mechanical forces of different levels and directions provided by BME with different concentrations could function accordingly in maintaining the undifferentiated state of stem cells or enhancing their differentiation [25]. BME offers a reliable feeder-free substrate for the attachment and has been extensively utilized in various studies to explore critical cellular processes such as adhesion, migration, proliferation, and other developmental aspects [27–29] in a range of stem cells, including human embryonic stem cells [30] and induced pluripotent stem cells [31]. In this study, we employed a stem cell qualified BME, formulated without growth factors, to negate any potential influence of these factors on stem cell differentiation. Utilizing this growth factor-free BME, we developed a 3D culture system designed to assess its impact on the properties of NSPs with potential applications in cochlear regeneration, examined *in vitro*.

In the current study, we first characterized the sphere forming capacity and neuron generation efficiency of mouse inner ear Sox10+ GCs as a progenitor population and investigated the effects of the BME-3D culture system on the proliferation and neuronal differentiation ability of Sox10+ GCs *in vitro*. We assessed the functional maturation of the newly generated neurons, including their electrophysiological properties and their ability to form connections with HCs, and evaluated the ability of the BME-3D culture system to protect the Sox10+ GCs-derived cells from ototoxic drug damage. Finally, the characteristics of the differentiated neuronal cells were identified via transcriptome sequencing analysis. Our study provided a possible efficient strategy for the SGN regeneration study *in vitro*.

2. Materials and methods

2.1. Animal breeding and genotyping

Sox10-creER mice (Stock no. 027651) and Rosa26-tdTomato reporter mice (Stock no. 007914) were purchased from Jackson Laboratory (Maine, USA). All transgenic mice were genotyped by polymerase chain reaction (PCR) using DNA isolated from toe clippings and primers listed in Supplementary Table 1. Wild-type (WT) C57BL/6 mice were purchased from the Animal Center of Shandong University (Jinan, China).

All experiments and procedures were approved by the Animal Care of Shandong University, China (No. ECAESDUSM 20123011) and adhered to the National Institutes of Health Guide for the Care and Use of Laboratory Animals.

2.2. Cochlear dissection and fluorescence-activated cell sorting (FACS)

The Sox10-creER mice were crossed with Rosa26 tdTomato mice to obtain Sox10/tdTomato double-positive (Sox10/tdTomato) littermates. The Sox10/tdTomato mice were treated with a single injection of 75 mg/kg tamoxifen (Sigma, USA) intraperitoneally at postnatal day (P) 0 to induce the Cre recombinase system and activate tdTomato fluorescence, and were sacrificed at P3. Briefly, after decapitation, the skulls of mice were cut along the midsagittal plane from the foramen magnum, and the temporal bones were placed in Hank's Balanced Salt Solution (Solarbio, China). The cochlear capsule was removed by fine forceps to expose the membranous labyrinth under a dissecting microscope, and the stria vascularis and the organ of Corti were removed the modiolus with the spiral ganglion was taken out. Collagenase type IV (1.5 mg/mL, Sigma) was used to digest the modiolus at 37 °C for 5 min, and fetal bovine serum (Gibco, USA) was added to terminate digestion. Culture medium was added to suspend the cells after centrifugation and pipetted up and down approximately 80–100 times to disrupt the tissue into single cells, and a 40-μm cell strainer (Corning, USA) was used to filter the single-cell suspension. Finally, dissociated cells from the ganglia were sorted on a BD FACS Aria III (BD biosciences, USA), and tdTomato+ and tdTomato− cells were collected separately.

2.3. Cell culture and drug treatment

FACS-isolated tdTomato + cells (2500 cells per well) were seeded in 96-well ultra-low attachment plates (Corning) in full medium (FM) or 1 % BME (Bio-Techne, USA). The composition of FM was as follows: B27 (1:50; Invitrogen, USA), N2 (1:100; Invitrogen), ampicillin (50 mg/mL; Sigma-Aldrich, USA), normocin (50 mg/mL; InvivoGen, USA), basic fibroblast growth factor (10 ng/mL; Sigma), epidermal growth factor (20 ng/mL; Sigma), heparan sulfate (50 ng/mL; Sigma), and insulin-like growth factor (50 ng/mL; Sigma) in Dulbecco's Modified Eagle medium/F12 (Invitrogen). The 1 % BME solution was prepared by adding 1 μL BME into 99 μL FM. For the cell proliferation experiment, 0.1 mg/g 5-ethynyl-2′-deoxyuridine (EdU; Invitrogen) was added into the culture medium to label the proliferating cells at DIV 5 for 4 h. After 5 days of expansion, neurospheres were collected and analyzed or treated with or without 60 μM cisplatin (Sigma-Aldrich) for 24 h. For the neuronal differentiation experiment, the collected neurospheres were digested using Accutase (Thermo Fisher, USA) and then plated on glass slides pre-

coated with laminin (Sigma) and ornithine (Sigma) in differentiation medium (DM) or 20 % BME. DM was supplemented with N2, B27, 50 mg/mL ampicillin, 50 mg/mL normocin, brain-derived neurotrophic factor (50 ng/mL; R&D Systems, USA), and neurotrophin-3 (50 ng/mL; R&D Systems). The 20 % BME solution was prepared by adding 20 μL BME into 80 μL DM. After 10 days of differentiation, cells on the glass slides were analyzed or treated with or without 30 μM cisplatin for 24 h. All cell culture procedures described above were conducted at 37 °C in a 5 % CO_2 incubator, with the medium replaced every 2 or 3 days.

2.4. Co-culture with cochlear HCs

The wholemount cochleae of P3 WT mice which removed the spiral ligament, stria vascularis, and modiolus, were dissected out following our previously published procedure [32,33], four cochlear explants were placed on each glass slide pre-coated with laminin, and ornithine overnight for allowing the cochlear HCs to attach to the glass slides. Cells after 10 days of neuronal differentiation in DM were digested and seeded at a density of 10000 cells per well to DM or 20 % BME for co-culture with the cochlear HCs. Newly formed SGN-HC connections were observed after 5 days of co-culture.

2.5. RNA extraction and RT-PCR

Total RNA was extracted using TRIzol reagent (Invitrogen), and RNA concentration was measured using a spectrophotometer (Bio-Rad, USA). The Revert Aid First Strand cDNA Synthesis Kit (Thermo Scientific, USA) was used to synthesize complementary DNA from corresponding RNA by reverse transcription, and SYBR Green Premix Ex Taq (Takara, Japan) was used to perform quantitative RT-PCR on a realplex PCR system (Eppendorf), with glyceraldehyde 3-phosphate dehydrogenase as the control gene. Differences in messenger RNA (mRNA) expression were assessed based on the comparative cycle threshold method. The primers used were listed in the Supplementary Table 1.

2.6. Cell viability detection

Cell Counting Kit-8 (CCK8) reagent (Sigma-Aldrich) was added (10 μL per 100 μL of culture medium) and was further incubated for 4 h at 37 °C. Cell viability was detected every day during expansion culture, on the 1st and 10th day during neuronal inducement culture, and also 24 h after cisplatin treatment. A Multiskan MK3 microplate reader (Thermo Fisher Scientific, USA) was used to measure the absorbance of the samples at 450 nm. The cell viability in different groups was compared to day 1 group.

2.7. Flow cytometry analysis

The collected neurospheres were digested into single cells using Accutase. For apoptosis detection, cell suspensions were processed using the Annexin V-FITC Apoptosis Detection Kit (Beyotime) and analyzed using a BD Accuri C6 Plus flow cytometer (BD Biosciences).

2.8. Cryosection

The cochleae of P3 mice were fixed with 4 % paraformaldehyde (PFA) overnight at 4 °C. The following day, the cochleae were dehydrated successively in 15 %, 20 %, and 30 % sucrose solutions and then quickly frozen in optimal cutting temperature compound (Sakura Finetek, USA) on dry ice. The frozen cochleae were sectioned into 10 μm slices using a cryostat (Leica CM 1850; Leica, Germany) or stored at −80 °C.

2.9. Immunofluorescence analysis

Neurospheres were collected after expansion culture and resuspended and washed twice in phosphate-buffered saline (PBS). The spheres were then fixed with 4 % PFA for 1 h and adhered to slides by cytocentrifugation at 800 g for 5 min in a cytospin (Thermo Fisher). After neuronal differentiation culture, the glass slides with newly generated neurons were immersed in PBS at 4 °C for 30 min to melt the BME and then fixed with 4 % PFA for 1 h. The samples obtained were then permeabilized in 0.25 % Triton X-100 for 15 min and immersed in blocking solution for 1 h at room temperature, followed by incubation with the appropriate primary antibodies, i.e., Anti-Tuj1 (1:500; Abcam, UK), anti-NeuN (1:1000; Cell Signaling Technology, USA), anti-Sox10 (1:1000; Abcam), anti-Hmga2 (1:600; Cell Signaling Technology), anti-Sox2 (1:400; Santa Cruz, USA), anti-Hmgb2 (1:1000; Abcam), anti-Nestin (1:1000; Abcam), or anti-synaptophysin (1:1000, Sigma), at 4 °C overnight. Thereafter, the samples were incubated with secondary antibodies (1:1000; Invitrogen), along with DAPI (1:1000, Invitrogen) or phalloidin (1:1000, Invitrogen) for 1 h at room temperature. The prepared slides were examined using a laser scanning confocal microscope (Leica STELLARIS 5; Leica, Germany). This examination involved capturing confocal images with a 40x objective lens in XYZ acquisition mode. The images were taken with a 0.5 μm z-step size between each optical section at Z-Stack. For detailed analysis, we utilized the "3D visualization module" of the LAS X software to generate 3D reconstructions of the immunofluorescence images from these confocal data, allowing for a comprehensive and accurate visualization of the samples.

Apoptosis was assessed based on DNA fragmentation using the Click-iT Plus TUNEL Assay Kit for In Situ Apoptosis Detection (Invitrogen) according to the manufacturer's instructions.

2.10. Patch-clamp electrophysiological recordings

The electrophysiological properties of P3 mice native SGNs and the newly generated neurons were assessed using whole-cell patch-clamp recordings. The neurons were washed and then bathed in a solution with the following composition: (all values in mM) 130 NaCl, 2.5 KCl, 2.5 $CaCl_2$, 1.3 $MgCl_2$, 10 HEPES, 10 glucose; osmolarity, 310 mOsm; pH 7.4). The recording pipettes were filled with a solution with the following composition: (all values in mM) 130 potassium gluconate, 5 HEPES, 0.5 EGTA, 2 $MgCl_2$, 0.1 $CaCl_2$, and 5 Na2-ATP; osmolarity, 300 mOsm; pH 7.2). An EPC10 (HEKA, Germany) patch-clamp amplifier was used for data acquisition, and action potentials were triggered by somatic current steps (duration, 10 ms) at intervals of 1s and in increments of 10 pA. The data was finally analyzed using PatchMaster v.2 × 73.5 (HEKA).

2.11. RNA-seq analysis

The total RNA of differentiated cells was extracted using Trizol reagent (thermofisher) following the manufacturer's procedure. The total RNA quantity and purity were analyzed with Bioanalyzer 2100 and RNA 6000 Nano LabChip Kit (Agilent, CA, USA), high-quality RNA samples with RIN number >7.0 were used to construct sequencing library. After two rounds of purification, the mRNA was fragmented into short fragments using divalent cations under elevated temperature (Magnesium RNA Fragmentation Module (NEB, USA) under 94 °C 5–7min). Then the cleaved RNA fragments were reverse-transcribed to create the cDNA by SuperScript™ II Reverse Transcriptase (Invitrogen, USA), which were next used to synthesize U-labeled second-stranded DNAs with *E. coli* DNA polymerase I (NEB, USA), RNase H (NEB, USA) and dUTP Solution (Thermo Fisher, USA). The size selection was performed with AMPureXP beads, and the ligated products were amplified with PCR for 8 cycles. The average insert size for the final cDNA libraries was 300 ± 50 bp. At last, we performed the 2 × 150 bp paired-end sequencing (PE150) on an Illumina Novaseq™ 6000 following the vendor's recommended protocol and then aligned reads of all samples to the reference genome using HISAT2.

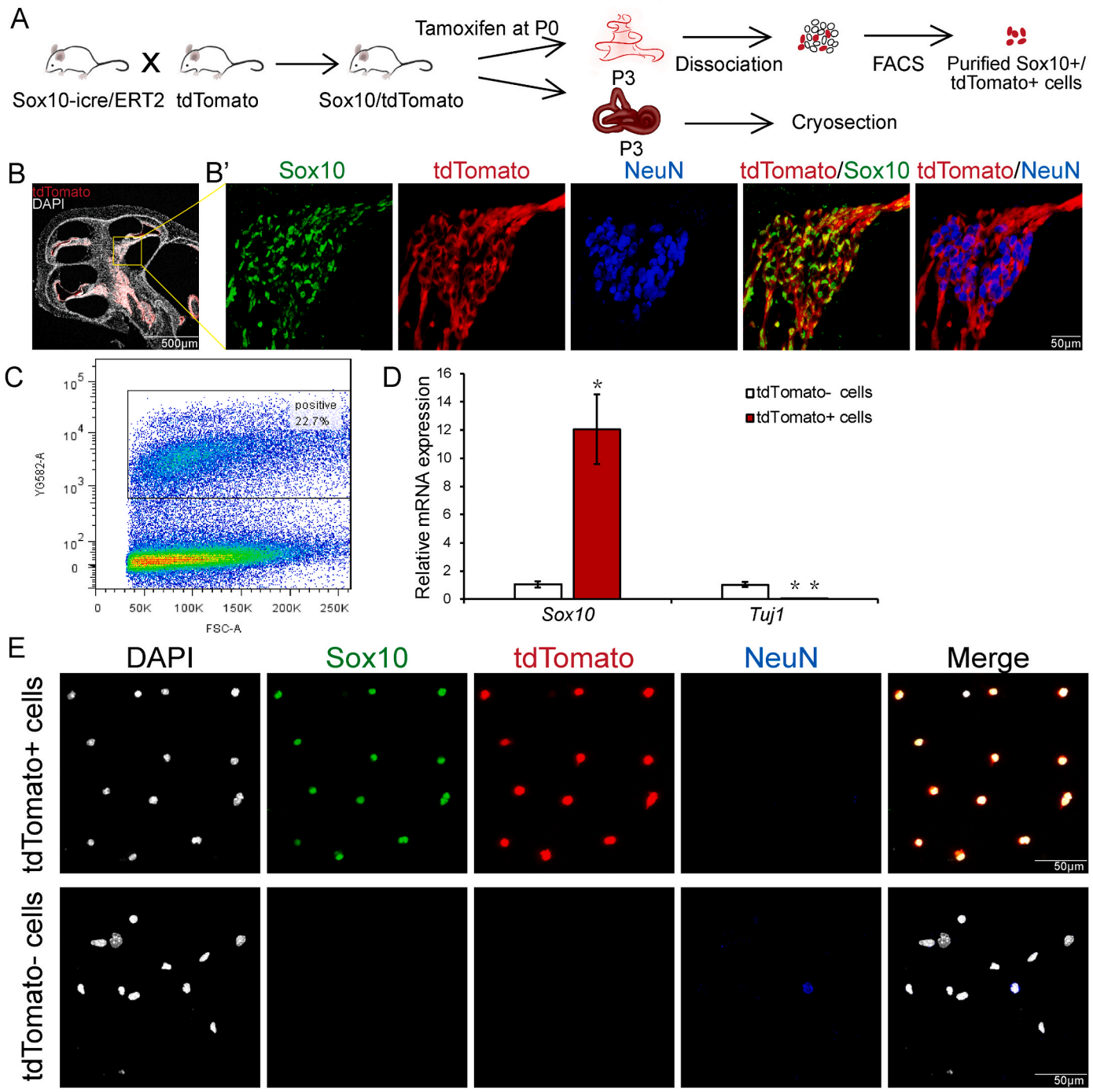

Fig. 1. Isolation and characterization of mice inner ear Sox10+ GCs. (A) Simplified diagram of the experimental process. Sox10/tdTomato mice were treated with tamoxifen at P0–P1 and sacrificed at P3. The cochlear modiolus was dissociated into single cells, and Sox10+ cells were isolated and collected using FACS; **(B–B')** Representative images of the cochlear cryosections from P3 Sox10/tdTomato mice labeled with DAPI (grey), tdTomato (red), Sox10 (green) and NeuN (blue). **(C)** tdTomato + cells were isolated from dissociated modiolus cells via FACS. **(D)** RT-PCR results showed that the collected tdTomato + cells expressed a much higher mRNA level of Sox10 and an extremely low mRNA level of Tuj1 compared to those in tdTomato-cells. **(E)** Representative images of the collected tdTomato+ and tdTomato-cells labeled with DAPI, Sox10, tdTomato, and NeuN. n = 7 cells per group. Data were shown as the mean ± SEM. $^{**}p < 0.01$.

Genes differential expression analysis was performed by DESeq2 software between two different groups. The genes with the parameter of false discovery rate (FDR) below 0.05 and absolute fold change ≥2 were considered differentially expressed genes. Differentially expressed genes (DEGs) were then subjected to enrichment analysis of GO functions and KEGG pathways.

2.12. Image analysis

Confocal images of SGNs were taken using a Leica SPE confocal microscope and were analyzed with the ImageJ software V1.8.0 to evaluate the sphere number, sphere diameter, cell number, the longest neurite length (LNL), growth cone area, and synaptic puncta separately. Neurite length was measured from the body of the neuron to its farthest extension, and the length of the longest neurite of each newly generated

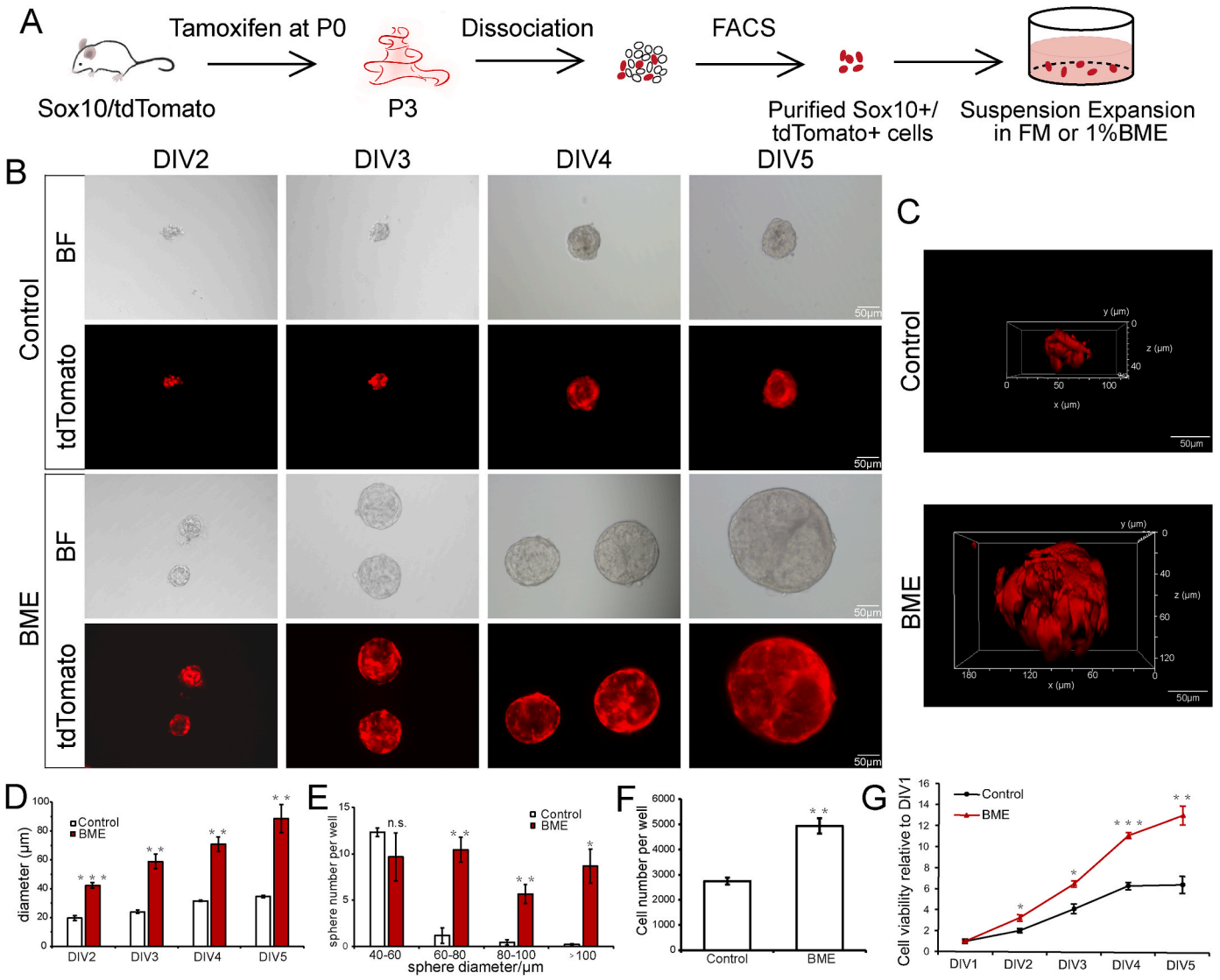

Fig. 2. BME-3D culture system promoted the sphere-forming ability of Sox10+ GCs. (A) The isolated Sox10+ GCs from P3 Sox10/tdTomato mice cochlea were cultured to form neurospheres in a traditional 2D culture system or the BME-3D culture system for 5 days. **(B)** Bright-field (BF) and fluorescence images (tdTomato, red) of neurospheres cultured in the two different suspension systems on DIV 2–5; **(C)** 3D reconstructed immunofluorescence images of neurospheres in the two culture systems at DIV5. **(D)** Quantification of neurosphere diameter from DIV 2 to DIV 5 (all neurospheres in 6 wells of a 96-well plate for each group); **(E)** Quantification of neurosphere number per well (n = 6 wells of a 96-well plate for each group); **(F)** Quantification of the cell number per well determined using flow cytometry after dissociating the neurospheres into single cells (n = 6 wells of a 96-well plate for each group); **(G)** CCK8 assay results showed the cell viability of each group. Data were shown as the mean ± SEM. $*p < 0.05$, $**p < 0.01$, $***p < 0.001$.

neuron was defined as the LNL, which was recorded as 0 if there were no neurites. For each experiment, the average values in each group were obtained using at least six samples.

2.13. Statistical analysis

Statistical analyses were conducted using SPSS 25.0 software. Two-tailed, unpaired Student's t-tests were used to determine statistical significance when comparing two groups. One-way ANOVA followed by Bonferroni's multiple comparisons test were used for comparing multiple groups. All experiments were repeated at least three times, data were presented as the mean ± SEM (standard error of the mean). A value of $p < 0.05$ was considered to be statistically significant.

3. Results

3.1. Isolation and characterization of mouse inner ear Sox10+ GCs

Previous studies have proved that Sox10 was expressed in the epithelium of the cochlear duct, spiral ganglion, and vestibule at P1, and Sox10-expressing cells were GCs in the spiral ganglion [9,34]. In this study, we first identified the expression of Sox10 and the labeling of tomato fluorescent in the cochlear spiral ganglion in Sox10/tdTomato mice (Fig. 1A). Sox10 and NeuN was used as the GC marker and SGN marker separately, the immunofluorescence images of cochlear cryosection (Fig. 1B') showed that tdTomato fluorescence was clustered at the cochlear duct, spiral ganglion, and modiolus in the cochleae of P3 Sox10/tdTomato mice. As shown in the high magnification image, almost all tdTomato fluorescence was specifically co-localized with Sox10+ cells, but not with NeuN + cells (Fig. 1B), indicating that the GCs, but not SGNs, were labeled with tdTomato fluorescence in the P3 mice cochlea.

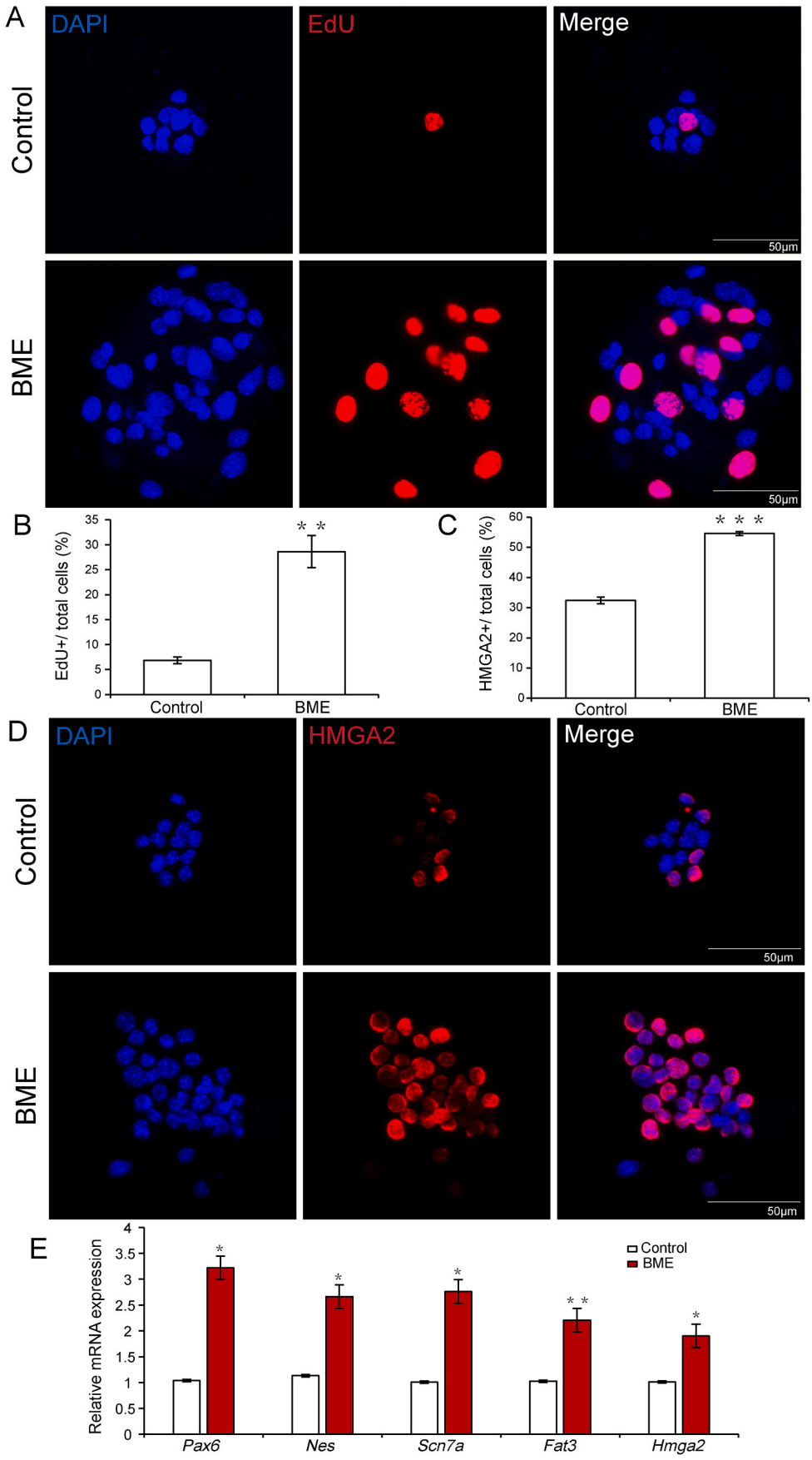

(caption on next page)

Fig. 3. The BME-3D culture system enhanced the proliferation ability and stem cell-related properties of Sox10+ GCs. The isolated Sox10+ GCs from P3 Sox10/tdTomato mice cochlea were cultured to form neurospheres in a traditional 2D culture system or the BME-3D culture system for 5 days. **(A)** Immunofluorescence images of neurospheres after the 4 h EdU pulse experiment at DIV5. **(B)** Quantification of EdU-positive cells/total cells per neurosphere at DIV 5 (n = 6 neurospheres in each group). **(C, D)** Immunofluorescence images of neurospheres stained with Hmga2 at DIV 5 and the percentage of Hmga2+ cells/total cells per neurosphere (n = 6 neurospheres in each group). **(E)** The mRNA expression levels of stem cell-related genes in the BME-3D culture system and control group at DIV 5. Results were normalized to the values for *Gapdh*. Data were shown as the mean ± SEM. $^{*}p < 0.05$, $^{**}p < 0.01$, $^{***}p < 0.001$.

Using fluorescence-activated cell sorting (FACS), we then separated tdTomato+ and tdTomato-cells from the cochlea of P3 Sox10/tdTomato mice. The tdTomato + cells comprised approximately 22.7 % of all cells collected (Fig. 1C). Quantitative RT-PCR analysis showed that *Sox10* mRNA expression in tdTomato + cells was about 12 times higher compared to tdTomato-cells, while *Tuj1* mRNA levels were significantly lower in the tdTomato + group (Fig. 1D). Immunofluorescence studies indicated that all tdTomato + cells were also positive for Sox10, with none of the tdTomato + cells exhibiting co-labeling with NeuN. Among the isolated tdTomato + cells, the proportion of Sox10-positive cells to the total cell count (stained with DAPI) was 88.31 % ± 1.50 %. Conversely, tdTomato-cells showed no Sox10 positivity (Fig. 1E). These findings confirmed that the isolated tdTomato + cells were a highly purified population of Sox10+ GCs, devoid of SGN contamination.

3.2. BME-3D culture system promoted the sphere-forming ability of Sox10+ GCs

To investigate the neurosphere-forming ability of Sox10+ GCs *in vitro*, the isolated tdTomato + cells from P3 Sox10/tdTomato mice were cultured for proliferation in a traditional suspension culture system (control group) or the BME-3D culture system (BME group) for 5 days (Fig. 2A). Bright-field (BF) and fluorescence (tdTomato, red) imaging showed that tdTomato + cells began forming neurospheres in both culture systems by day 2 *in vitro* (DIV2). The 3D immunofluorescence reconstructions showed that, by DIV 5, neurospheres in the BME group were significantly larger than those in the control group (Fig. 2B and C). Statistical analysis showed that the diameter of neurospheres in the BME group was approximately 2.55 times larger than that in the control group (88.44 ± 9.64 μm vs. 34.68 ± 0.82 μm; $P < 0.01$; Fig. 2D). The number of neurospheres per well was counted and no significant difference was found between the two groups in diameter range of 40–60 μm; however, the number was increased markedly in the BME group compared to the control group in the diameter range of 60–80 μm and larger (Fig. 2E). Furthermore, the total number of cells per well was significantly higher in the BME group than in the control group after 5 days of sphere-forming culture (4937.54 ± 303.29 vs. 2748.46 ± 134.76; $P < 0.01$; Fig. 2F). The viability of the cultured cells, as determined using CCK8 analysis, was also found to be more than twice as high in the BME group as that in the control group (Fig. 2G).

3.3. Proliferation ability and stem cell-related properties of Sox10+ GCs were enhanced in the BME-3D culture system

To further determine the proliferative ability of Sox10+ GCs, EdU was added in the proliferation culture medium 4 h before harvest at DIV 5. The percentage of EdU + cells/DAPI + cells, i.e., the newly proliferated cells per neurosphere, within the 4 h period, was almost 4 times higher in the BME group than that in the control group (28.63 % ± 3.23 % vs. 6.85 % ± 0.70 %; $P < 0.01$; Fig. 3A–B), indicating that the proliferation ability of Sox10+ GCs was promoted in the BME-3D culture system.

During sphere-forming culture, inner ear GCs de-differentiated into neuronal progenitor-like cells capable of regenerating neurons [7,35]. To address whether the BME-3D culture system enhanced the GCs' ability to revert to a stem cell-like state, we assessed the expression of Hmga2, a critical transcription factor for neural stem cells and pro-sensory cells in the cochlea [36], at day 5 of the culture. We observed a significantly higher percentage of Hmga2+ cells per neurosphere in the BME group compared to the control group (54.57 % ± 0.65 % vs. 32.42 % ± 1.14 %; $P < 0.001$; Fig. 3C–D). In additin, we noted a marked upregulation of several other neural stem cell markers in the BME group (Supplementary Fig. 1). These markers include Sox2 and Nestin, both integral in maintaining the optic neuronal progenitor (ONP) stage and preventing differentiation into neurons [37] as well as Hmgb2, which is associated with the activation and proliferation of a subset of neural stem cells [38]. Furthermore, RT-PCR results showed that the mRNA expressions of the neural stem cell-specific genes *Pax6, Nes, Scn7a, Fat3,* and *Hmga2* were all up-regulated in the BME group compared to the control group (Fig. 3E). These results suggested that the stem cell-related properties of progenitor GCs were enhanced in response to the BME-3D culture system.

3.4. The neuronal differentiation capacity of Sox10+ GCs was increased in the BME-3D culture system

To explore whether the BME-3D culture system could be conducive to the process of neuronal differentiation, neurospheres were digested into single cells and then cultured in DM (Control group) or with 20 % BME (BME group) for 10 days (Fig. 4A). Cells were harvested for immunostaining analysis, Tuj1 was used to label the newly generated neurons, the tdTomato and Tuj1 double positive (Tuj1+ tdTomato+) cells were both observed in the two culture systems, indicating the newly generated neurons derived from Sox10+ GCs. Cell counting analysis showed that the percentage of Sox10+ GC-derived neurons (Tuj1+ tdTomato + cells/total tdTomato + cells) was significantly increased in the BME group compared to that in the control group (74.67 % ± 2.22 % vs. 55.66 % ± 2.68 %; $P < 0.01$; Fig. 4B–C), suggesting that the BME-3D culture system improved the neuronal differentiation efficiency of inner ear Sox10+ GCs. Neurite outgrowth was also examined by measuring the LNL, the longest neurite length from the body of the neuron to its farthest extension, of newly generated neurons. It showed that the LNL of newly generated neurons in the BME group was raised to 2.77-fold of that in the control group (352.74 ± 19.74 vs. 127.97 ± 7.77 μm; $P < 0.001$; Fig. 4D–E). The 3D reconstruction of immunofluorescence images revealed the spatial growth of the newly generated neurons (Fig. 4F). Furthermore, we observed that the mRNA expression levels of the pan-neuronally expressed gene *Tuj1*, the SGN-specific genes *Gata3, Prox1,* and *Scrt2,* as well as the neurogenesis-related genes *NeuroD1* and *Ascl1* were all significantly increased in the BME group than in the control group (Fig. 4G–H).

3.5. The BME-3D culture system promoted the growth of neurites and the maturation of the newly generated neurons

The newly generated neurons were labeled with phalloidin and the growth cone areas were measured. The results showed that the average growth cone area was 15.08 ± 0.84 μm^2 in the BME group compared to the 9.31 ± 1.25 μm^2 in the control group (Fig. 5A–B), indicating that the expansion of the growth cone was accelerated in the 3D culture system and that neurite outgrowth was therefore promoted. To compare the synaptic vesicle densities of the newly generated neurons, we detected the expression of synaptophysin, a major synaptic vesicle intrinsic membrane protein [39], in neurites. As illustrated in Fig. 5C–D, the synaptic vesicle density in the BME group was much higher than that in the control group (10.38 ± 0.18 vs. 6.36 ± 0.76 per 10 μm neurite; P <

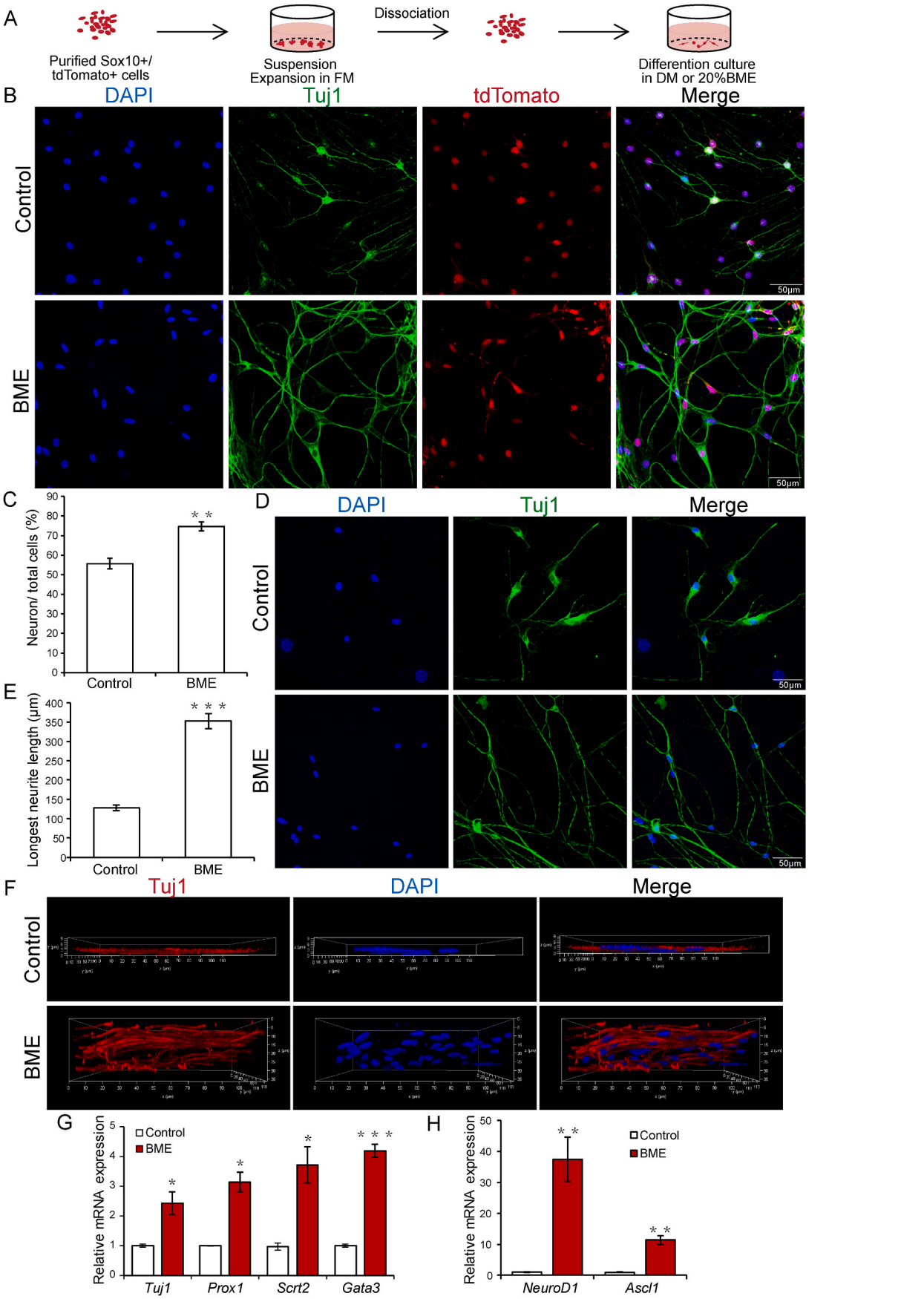

(caption on next page)

Fig. 4. The neuronal differentiation capacity of Sox10+ GCs was promoted in the BME-3D culture system. (A) The neurospheres generated from Sox10+ GCs were digested into single cells and then cultured in traditional DM or 20 % BME for 10 days neuronal differentiation culture. **(B)** Immunofluorescence images of the newly generated neurons labeled with Tuj1 (green), tdTomato (red), and DAPI (blue). **(C)** The percentage of Sox10+ GC-derived neurons (Tuj1+ tdTomato + cells/total tdTomato + cells, n = 6 fields in each group). **(D)** Immunofluorescence images of neurites of the newly generated neurons labeled with Tuj1. **(E)** Statistical analysis of the longest neurite length of the newly generated neurons (n = all neurons in 6 fields in each group). **(F)** 3D reconstruction of immunofluorescence images revealed the spatial growth of the newly generated neurons. **(G–H)** The mRNA expression levels of the pan-neuronally expressed gene *Tuj1,* SGN-specific genes *Gata3*, *Prox1*, and *Scrt2,* as well as neurogenesis-related genes *NeuroD1* and *Ascl1* in the two culture system. Results were normalized to the values for *Gapdh*. Data were shown as the mean ± SEM. $^{*}p < 0.05$, $^{**}p < 0.01$, $^{***}p < 0.001$.

0.01). Altogether, these results indicated that BME application during the neuronal differentiation culture facilitated the growth of newly derived neurons.

Next, to determine the electrophysiological properties of the newly generated neurons, whole-cell patch-clamp recording was performed, and native SGNs isolated from P3 WT mice were used as positive controls (Fig. 5E). The newly generated neurons in each group were capable of firing action potentials (APs), and the threshold stimulus current in the BME group was significantly lower than that in the control group (38 ± 4 pA vs. 74 ± 4 pA), but there was no statistical difference in the threshold stimulus current between the BME group and P3 SGNs (36 ± 4 pA. P < 0.001; Fig. 5G). Furthermore, there was no statistical difference in the depolarization duration of APs in the BME-3D culture group and the control group (3.92 ± 0.24 ms vs. 4.82 ± 0.30 ms); however, the depolarization duration of APs in the BME-3D culture group resembled more that in P3 mice native SGNs (2.52 ± 0.20 ms; Fig. 5H). These results suggest that the electrophysiological characteristics of newly generated neurons in the BME-3D culture system mice more closely resembled those of native SGNs in newborn mice.

3.6. BME-3D culture system intensified the reinnervation of HCs with newly generated neurons derived from Sox10+ GCs

To determine whether the GC-derived neurons have the capacity to connect with HCs, which are the targets of native SGNs to form connections *in vivo*, cells after 10 days of neuronal differentiation in DM were digested and then co-cultured with the cochlear HCs. Newly formed SGN-HC connections were observed after 5 days of co-culture (Fig. 6A) in the 2D and 3D culture system. Immunofluorescence analysis showed that the neurites of newly generated neurons derived from Sox 10+ GCs (tdTomato + Tuj1+) were extended toward the HCs in both the control and BME groups (Fig. 6B). However, none of the newly generated neurons formed connections with HCs in the control group, whereas 2.14 ± 0.43 connections per cochlea HCs explant were formed in the BME group (Fig. 6C), suggesting that the BME-3D culture system enhances the capacity of Sox10+ GC-derived neurons to form connections with HCs, thus intensifying the reinnervation of HCs.

3.7. BME-3D culture system protected neurospheres and newly generated neurons from cisplatin-induced damage

To explore whether the BME-3D culture system protects neurosphere cells and newly generated neurons from ototoxic drug-induced damage, 60 μM cisplatin was added at DIV 5 of sphere-forming culture for 24 h. Cell viability was assessed using the CCK8 assay, and cell apoptosis was analyzed via TUNEL staining and flow cytometry analysis (Fig. 7A). The results of the CCK8 assay with neurospheres showed that the cell viability after cisplatin treatment was reduced to 66.16 % ± 3.51 % of untreated cells in the control group while it was increased to 85.44 % ± 1.72 % of untreated cells in the BME-3D group (Fig. 7B). The average percentage of TUNEL + cells per neurosphere was much lower in the BME group than in the control group (13.07 % ± 0.77 % vs. 30.17 % ± 1.44 %; P < 0.001; Fig. 7C–D). Consistent with the results of TUNEL staining, flow cytometry analysis with single cells digested from neurospheres revealed that the percentage of apoptotic cells was significantly down-regulated in the BME group than that in the control group (10.97 % ± 1.23 % vs. 31.91 % ± 2.35 %; P < 0.001; Fig. 7E–F).

The response of newly generated neurons to ototoxic drugs was also examined, 30 μM cisplatin was added to the differentiation culture system at DIV 10 and incubated for 24 h (Fig. 7G). CCK8 assay showed that the cell viability was reduced to 81.74 % ± 3.15 % of that without cisplatin treatment in the control group, whereas it was 98.21 % ± 4.86 % in the BME group (Fig. 7H). The percentage of TUNEL + -neurons (TUNEL + Tuj1+ cells/total Tuj1+ cells) in the BME group was much lower than that in control group (1.44 % ± 0.32 % vs. 8.13 % ± 0.11 %; P < 0.001; Fig. 7I–J). Taken together, these results indicated that the BME-3D culture system protected both neurospheres and newly generated neurons from cisplatin-induced damage.

3.8. Transcriptome changes of newly differentiated neurons induced by BME-3D culture system

Transcriptome sequencing analysis was performed to identify the characteristics of the differentiated cells in the BME group compared to control group after 10 days of neuronal differentiation culture. Compared with the control group, the expression levels of 1269 genes were significantly altered, including 677 up-regulated genes and 592 down-regulated genes, in the BME group (Fig. 8A). The GO enrichment analysis showed that the DEGs were mainly enriched in the terms related to cellular responses to culture environment as cell adhesion, response to mechanical stimulus; cell functional and physiological behavior as axon guidance, positive regulation of synaptic transmission, glutamatergic, synapse organization, calcium-mediated signaling; neuronal differentiation and maturation as regulation of cell differentiation, peripheral nervous system development, positive regulation of neuron projection development, perineuronal net (Fig. 8B). Consistently, the KEGG enrichment analysis suggested that the DEGs were enriched in ECM-receptor interaction, focal adhesion, calcium signaling pathway, neuroactive ligand-receptor interaction, axon guidance, etc. (Fig. 8C). Heatmap graph of the 60 representative DEGs of great significance in BME group compared to control group revealed that some critical DEGs associated with neuronal development (*Aatk*, *Nr4a1*, *Arc*, *Tubb4a*, *Itga7*, *Gas7*, *Slc8a3*, *Cacna1h*, *Adam11* and *Plxnd1*) and neuronal survival (*Zfp36* and *Trf*) were significantly upregulated in the BME-3D culture system (Fig. 8D). We further analyzed the representative differentially expressed transcription factors. Notably, some key transcription factors (*c-Jun, Dlx11*, *Gata2*, *Junb*, *Pou3f2*, *Foxd3*, *Zbtb16*, *Bhlhe22*, and *Prdm8*) that may play a role in neuronal differentiation and maturity were upregulated in the BME-3D group as well (Fig. 8E). qPCR was performed to confirm the mRNA expression levels of the interested DEGs (Fig. 8F).

4. Discussion

Regeneration of neural cells from endogenous cochlear NSPs may offer a future tool to restore the auditory circuit and to enhance the performance of cochlear implants, the hearing devices that transmit auditory information by electrically stimulating the residing SGNs to the brain [40]. A basic requirement for using the NSPs in animal models or clinical trials in the future is a detailed understanding of their characteristics. In this study, for the first time, we purified the Sox10+ GCs from mice spiral ganglions and identified them as inner ear progenitors that were able to form neurospheres and give rise to neurons *in vitro*. In the mammalian inner ear, Sox10 is expressed in all of the cells in the otic vesicle at embryonic 9.5, but it is absent in HCs, mesenchymal cells, or

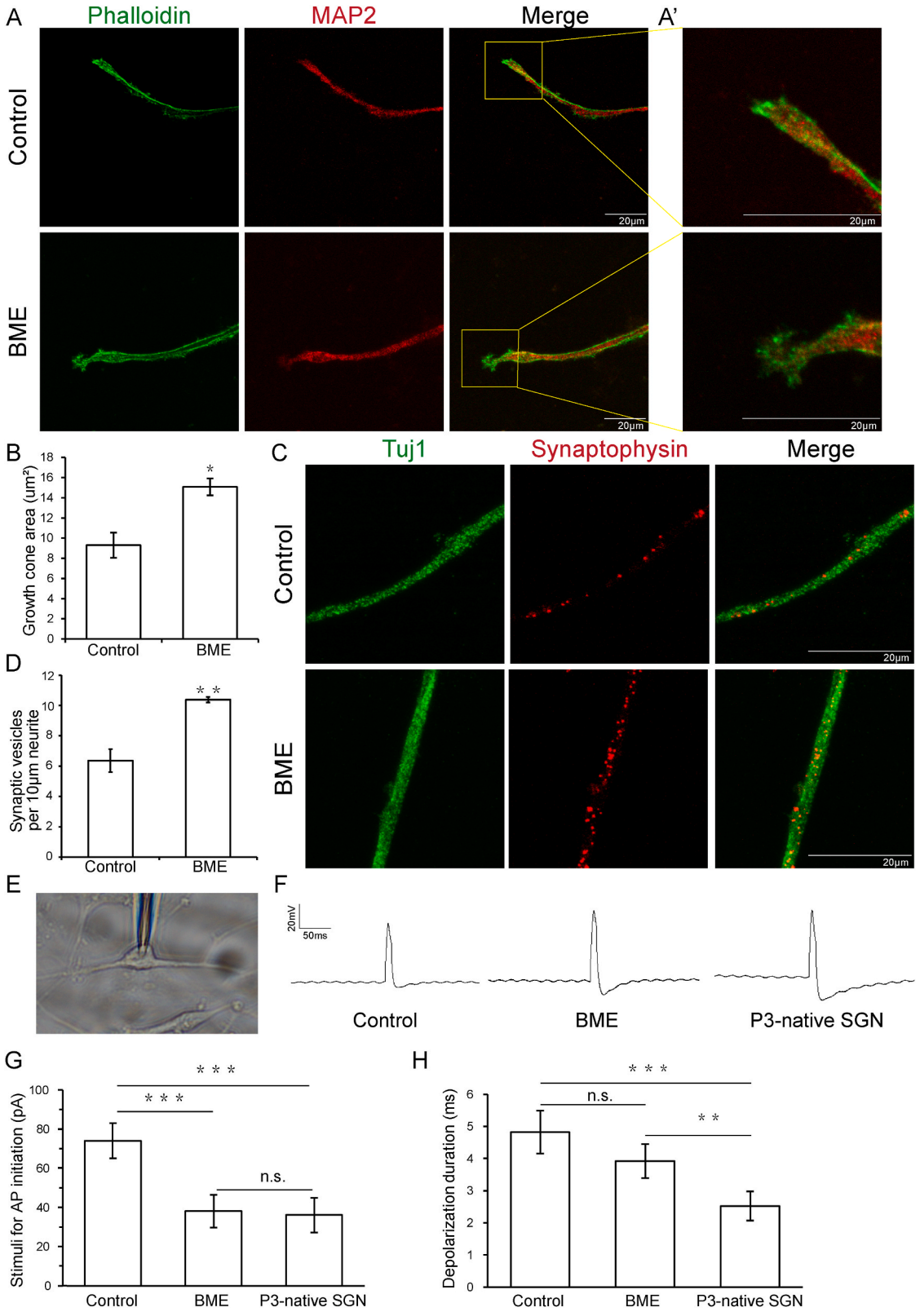

Fig. 5. The BME-3D culture system promoted the neurite growth and maturation of the newly generated neurons. The neurospheres generated from Sox10+ GCs were digested into single cells and then cultured in traditional DM or 20 % BME for 10 days. **(A)** Immunofluorescence images of growth cones stained with phalloidin (green), and neurites stained for MAP2 (red). **(B)** Quantification of the growth cone areas of the newly generated neurons (n = 6 neurites in each group). **(C)** Immunofluorescence images of synaptic vesicles stained with synaptophysin (red) and Tuj1 (green). **(D)** Quantification of synaptic vesicle density (n = 6 neurites in each group). **(E)** Representative images of newly generated neurons targeted for whole-cell patch-clamp recording. **(F)** Representative action potentials of the newly generated neurons cultured in the BME-3D culture system, 2D culture system, and native SGNs of P3 WT mice. **(G, H)** Statistical analysis of the stimuli for AP initiation or depolarization duration of neurons in the three groups (n = 5 neurons). Data were shown as the mean ± SEM. $*p < 0.05$, $**p < 0.01$, $***p < 0.001$.

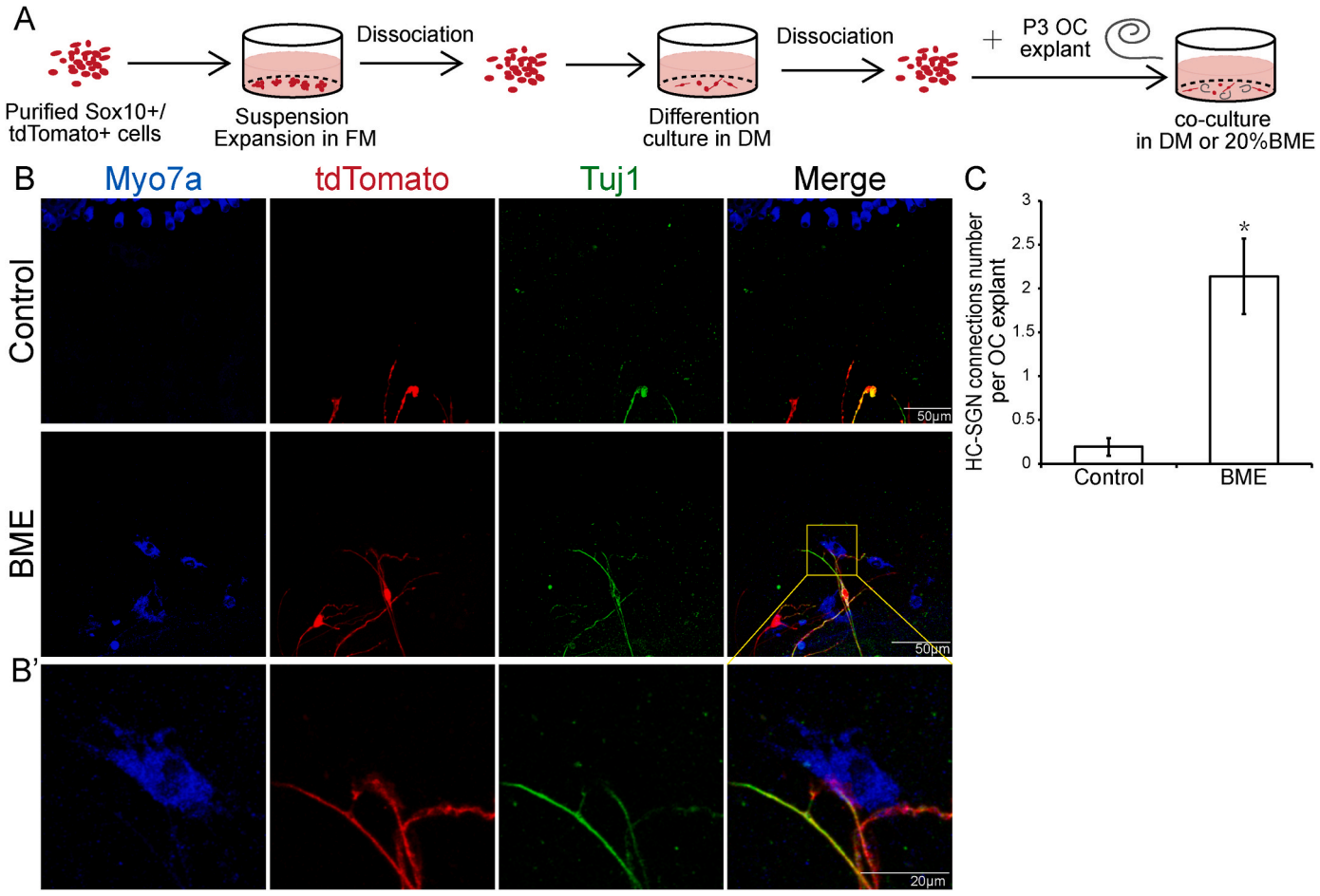

Fig. 6. BME-3D culture system intensified the reinnervation of HCs with newly generated neurons derived from Sox10+ GCs. (A) Cells after 10 days of neuronal differentiation in DM were digested and then co-cultured with the cochlear HCs in DM or 20 % BME for 5 days to observe the newly formed SGN-HC connections. **(B)** Immunofluorescence images showed the connections between the HC (Myo7a, blue) and newly-Sox10+ GC (tdTomato, red)-derived neurons (Tuj1, green) after the co-culture. **(C)** Statistical analysis the number of HC-SGN connections per OC explant (n = 3 or 4 OCs in each group). Data were shown as the mean ± SEM. $*p < 0.05$.

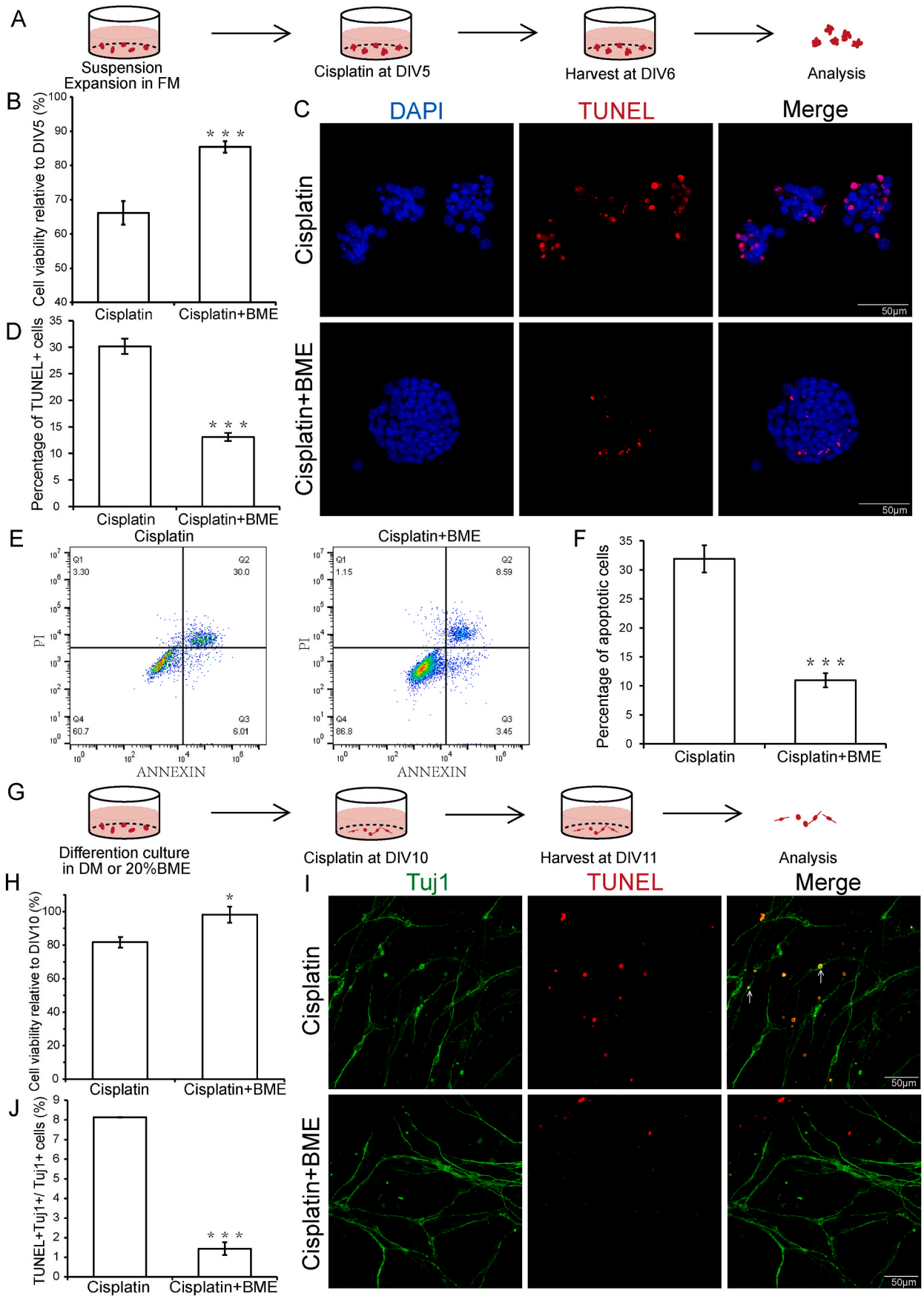

(caption on next page)

Fig. 7. BME-3D culture system protected neurospheres and newly generated neurons from cisplatin-induced damage. **(A)** Cisplatin (60 μM) was added at DIV 5 of sphere-forming culture and incubated for 24 h. **(B)** Cell viability was assessed using the CCK8 assay at DIV 6 of sphere-forming culture and normalized to that at DIV 5. **(C)** Immunofluorescence images of neurospheres treated with cisplatin for 24 h showed apoptotic cells labeled with TUNEL (red). **(D)** Quantification of the apoptotic cells/total cells in neurospheres treated with cisplatin (n = 6 neurospheres in each group). **(E)** Flow cytometry analysis of cells dissociated from the neurospheres after treatment with 60 μM cisplatin for 24 h. The population of apoptotic cells was Annexin V+/propidium iodide+. **(F)** The percentage of apoptotic cells/total cells in neurospheres treated with cisplatin. **(G)** Cisplatin (30 μM) was added at DIV 10 of differentiation-inducing culture and cells were harvested at DIV 11. **(H)** Cell viability determined using the CCK8 assay at DIV 11 of differentiation-inducing culture was normalized to that at DIV 10. **(I)** Immunofluorescence images of newly differentiated neurons (Tuj1, green) treated with cisplatin for 24 h showed apoptotic cells labeled with TUNEL (red). **(J)** Quantification of the apoptotic cells/total cells in differentiated-culture system treated with cisplatin (n = 6 wells in each group). Data were shown as the mean ± SEM. $*p < 0.05$, $**p < 0.01$, $***p < 0.001$.

SGNs after birth at P1 and only expressed in spiral ganglion GCs [34]. Sox10 is recognized as a marker of neural crest stem cells, and our study identified the cochlear Sox10+ GCs as a potential type of NSPs to generate SGNs *in vitro*.

Most current protocols utilize 2D culture methods for the neuronal differentiation of SGNs, which may not adequately mimic SGN development and function [41,42]. To address this, we developed an *in vitro* 3D culture system using BME of reduced growth factors. This system aimed to foster neural development through its inherent physical properties and spatial configuration, minimizing the potential confounding effects of undefined growth factors on neuronal differentiation. Our findings indicated that the BME-3D culture environment enhanced the proliferative capacity of Sox10+ GCs via mitosis, augmented stem cell-related characteristics of GCs, and significantly improved their neuronal differentiation efficiency and neurite growth. This enhanced performance was likely due to the 3D microenvironment created by BME, which provided mechanical and biochemical stimuli more akin to *in vivo* conditions than traditional 2D culture systems. Instead of the equal distribution of soluble factors in the traditional 2D homogeneous culture environment, BME-3D system could restrict the free diffusion of exogenous and autocrine cytokines as well as form sustained spatial gradients, which are more conducive to intercellular communication and behavioral regulation [43]. In addition, adhesions are formed on all surfaces of cells in the 3D culture system rather than only on one side in contact with the culture plate in the conventional system [44]. Integrin-mediated adhesions could establish intracellular cytoskeletal connections to the ECM and play a role in mechanotransduction between the cells and the ECM [45]. Multidirectional integrin binding was found to be more favorable for the formation of actin-rich stretches in cells in previous studies [46], which is consistent with our results that BME promotes neurite outgrowth.

Achieving functional maturity of newly generated neurons is one of the technical difficulties for their potential clinical application, studies have demonstrated that the application of BME can maintain the differentiated state of neurons and promote their functional maturation [47]. Our results also show that the synaptic vesicle density in the axons of newly generated neurons in the BME-3D culture system was significantly increased and the evoked APs are closer to those of P3 mouse native SGNs. It is worth noting that the formation of auditory circuits between newly generated neurons and HCs is a pivotal step in SGN regeneration, as for the functioning of the auditory afferent system relies on the ability of the neurons to recognize and connect to HCs [48]. Here, the co-culture results showed that the newly generated neurons in both conventional 2D culture and the BME-3D culture system extended toward HCs, but only the derived-neurons in the BME group formed connections with HCs after 10 days of neuronal differentiation culture. These results indicate that the newly generated neurons might be more functionally mature, as they tend to form auditory circuits with HCs, besides gaining longer axons in the BME-3D environment. However, whether the derived neuron-HC connections have physiological functions still needs further analysis.

Another finding of our study is that the BME-3D culture system protected proliferated cells and the newly derived neurons from cisplatin, a common ototoxic drug in clinical practice [49], induced apoptosis. Previous studies are consistent with our findings that BME can promote stem cell survival [50], and protect cells from apoptosis to varying degrees in the *in vitro* culture of other tissues [51,52]. The molecular mechanisms by which the BME-3D culture system guard against cisplatin-induced damage remain unclear. Previous research has indicated that reducing TNF-α release and expression can alleviate SGN inflammation and injury induced by cisplatin [53]. Our earlier studies have also demonstrated that activation of the Wnt signaling pathway reduced cisplatin-induced SGN damage by inhibiting caspase-associated apoptosis [54] Additionally, the PI3K/AKT signaling pathway has been shown to protect SGNs and HCs from cisplatin damage [32,55]. Our transcriptome sequencing analysis and subsequent KEGG pathway investigation revealed significant enrichment of these signaling pathways and molecules in the BME group. This suggests that they might be modulated within the BME-3D culture environment, and thus playing important roles in protecting neurospheres and newly differentiated neurons from cisplatin-induced ototoxicity.

BME provides complex and interdependent cues that affect cell signaling, gene expression, and regulation of cell behavior [56]. Our GO enrichment analysis revealed that terms enriched in the BME group are primarily related to the culture environment, including cell adhesion, response to mechanical stimulus, and ECM receptor interaction. For instance, CHL1, a cell adhesion molecule known for mediating extracellular interactions with other adhesion molecules and intracellular connections to cell surface receptors and scaffold proteins, was significantly upregulated in the BME group [57]. This molecule is also crucial for neurite outgrowth and synaptic plasticity [57]. Additionally, we observed an increase in the cell adhesion receptor ITGB4, which is typically expressed in neurons cultured in a 3D scaffold. ITGB4 mediates the interaction between laminin and neurons, facilitating neuronal spreading and network formation [58]. The upregulation of ITGB4 following BME-3D culture suggests its potential role in enhancing the neuronal differentiation of Sox10+ GCs within this system. Evidence also showed that the biological processes, such as neuronal development, axon guidance, synapse and ion channel activity were all enhanced in the BME system. Correspondingly, neuronal differentiation-related genes *Aatk* [59] and *Nr4a1* [60], axon growth-related genes *Arc* [61], *Tubb4a* [62], *Itga7* [63] and *Gas7* [64], electrophysiological activity-related genes *Slc8a* [65] and *Cacna1h* [66], synapse formation-related genes *Adam11* [67] and *Plxnd1* [68], and neuroprotection-related genes *Zfp36* [69] and *Trf* [70] were all significantly upregulated, which matches the relative alteration of the functional behavior of induced neurons. In addition, the transcription factor c-Jun, which is known for its role in neuronal differentiation and survival both *in vitro* and *in vivo* [71–73], was significantly upregulated in the BME group, thus suggesting its contribution to mechano-signaling and neuronal differentiation in the BME-3D culture system. The various genes with altered expression profiles in this system are likely pivotal and warrant further investigation.

Beyond *in vitro* applications, BME has shown potential for *in vivo* tissue engineering, regeneration, and repair. For instance, BME injected into rat hearts post-myocardial infarction recruited stem cells, influenced their differentiation and aided myocardial tissue repair [74]. Additionally, hydrogel introduced into the scala tympani through the round window had demonstrated potential for enhancing cochlear implant (CI) performance [21]. Here, our findings establish the BME-3D

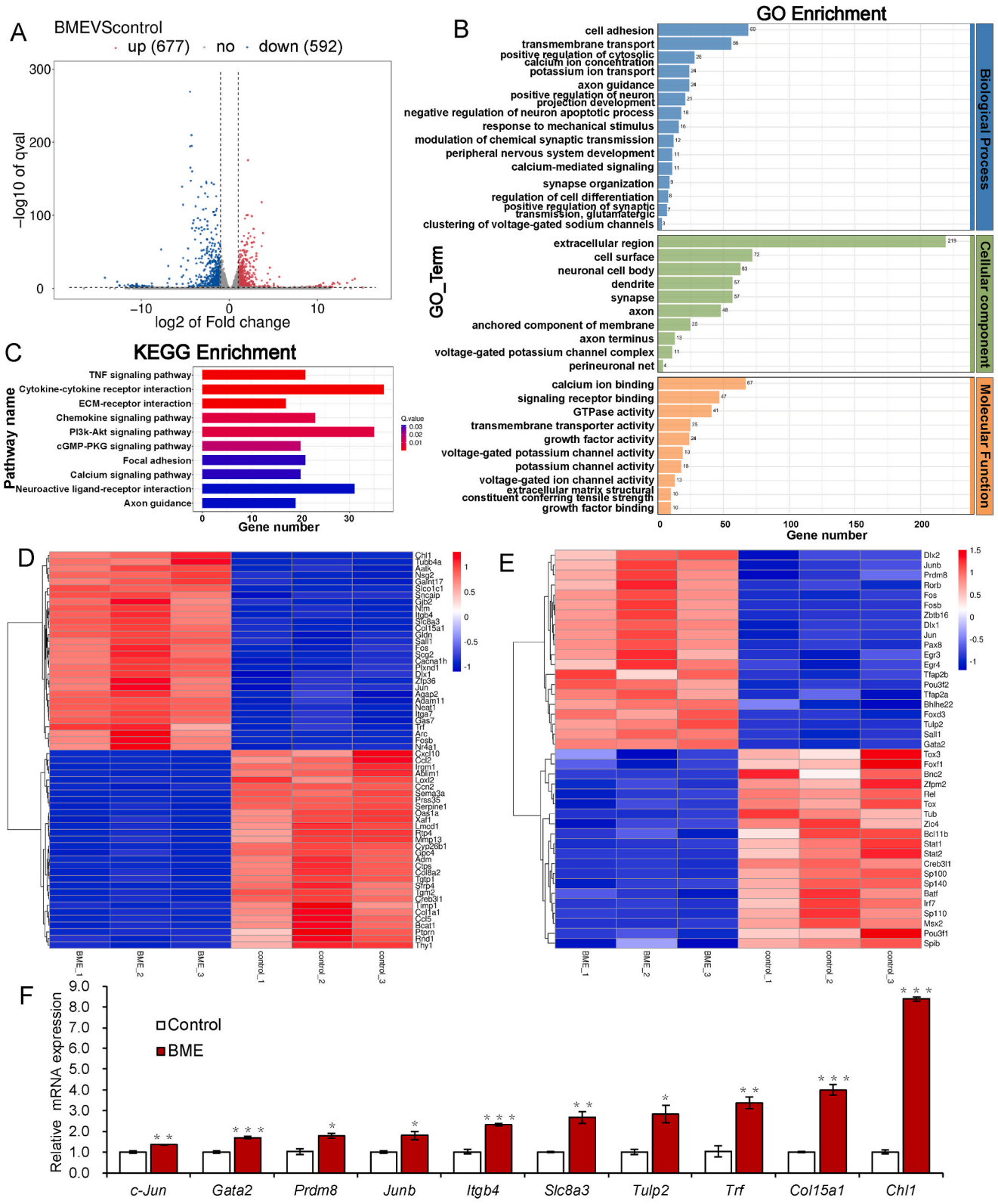

Fig. 8. Transcriptomic analysis of differentiated cells induced by BME-3D culture system. The neurospheres generated from Sox10+ GCs were digested into single cells and then cultured in traditional DM or 20 % BME for 10 days, then cells were collected for transcriptome sequencing analysis. **(A)** Volcano graph of DEGs in BME group compared to control group. The genes with the parameter of false discovery rate below 0.05 and absolute fold change ≥2 were considered DEGs. **(B)** GO enrichment analysis of DEGs in BME group compared to control group. The bar plot shows 35 representative enrichment GO terms. **(C)** KEGG enrichment analysis of DEGs in BME group compared to control group. The barplot shows 20 representative enrichment pathways. **(D)** Heatmap graph of the 60 representative DEGs of great significance in BME group compared to control group. **(E)** Heatmap graph of the 40 representative differentially expressed transcription factors extracted from DEGs in BME group compared to control group. **(F)** The mRNA expression levels of the interested DEGs confirmed by qPCR. Results were normalized to the values for *Gapdh*. Data were shown as the mean ± SEM. $*p < 0.05$, $**p < 0.01$, $***p < 0.001$.

culture system as a maneuverable tool for inner ear research *in vitro,* particularly for exploring SGN regeneration from stem cells. Given its excellent histocompatibility and biosafety, BME-based biomaterials could advance in *in vivo* studies, including promoting SGN regeneration in situ, enhancing cochlear implantation effects, and addressing SNHL clinical treatments following SGN injury, etc.

In conclusion, the BME-3D culture system developed in this study improved the proliferation capacity and neuronal differentiation efficiency of cochlear Sox10+ GCs and enhanced the functional maturation of newly generated neurons. The BME-3D culture system also intensified the reinnervation of newly generated neurons with HCs and protected the derived-cells from ototoxic drug damage. Thus, the BME-3D culture system could help to explore the mechanisms underlying the process of GCs-derived SGN regeneration, so as to lay the foundation for *in vivo* application of regenerated SGNs derived from cochlear GCs.

CRediT authorship contribution statement

Junze Lu: Conceptualization, Data curation, Methodology, Writing – original draft. **Man Wang:** Formal analysis, Investigation, Methodology, Writing – original draft. **Xue Wang:** Investigation, Methodology, Project administration, Software. **Yu Meng:** Investigation, Resources, Software, Validation. **Fang Chen:** Investigation, Methodology, Software, Validation. **Jinzhu Zhuang:** Formal analysis, Project administration, Validation. **Yuechen Han:** Investigation, Project administration, Validation, Visualization. **Haibo Wang:** Data curation, Funding acquisition, Investigation, Resources, Software, Supervision, Writing – original draft. **Wenwen Liu:** Conceptualization, Data curation, Funding acquisition, Project administration, Supervision, Writing – original draft, Writing – review & editing.

Declaration of competing interest

The authors declare that they have no known competing financial interests or personal relationships that could have appeared to influence the work reported in this paper.

Data availability

Data will be made available on request.

Acknowledgment

This work was supported by the National Natural Science Foundation of China (No. 82271176, 82271172, 82201290), the Major Program of National Natural Science Foundation of China (No. 82196821), the Major Fundamental Research Program of the Natural Science Foundation of Shandong Province (ZR2020ZD39, ZR2021ZD40), the Taishan Scholars Program of Shandong Province (No. tsqn201909189, ts20130913).

Appendix A. Supplementary data

Supplementary data to this article can be found online at https://doi.org/10.1016/j.mtbio.2023.100937.

References

[1] M. Wang, Y. Han, X. Wang, S. Liang, C. Bo, Z. Zhang, et al., Characterization of EGR-1 expression in the auditory cortex following kanamycin-induced hearing loss in mice, J. Mol. Neurosci. 71 (11) (2021) 2260–2274, https://doi.org/10.1007/s12031-021-01791-0.

[2] M. Wang, L. Xu, Y. Han, X. Wang, F. Chen, J. Lu, et al., Regulation of spiral ganglion neuron regeneration as a therapeutic strategy in sensorineural hearing loss, Front. Mol. Neurosci. 14 (2021) 829564, https://doi.org/10.3389/fnmol.2021.829564.

[3] S. Kanzaki, M. Toyoda, A. Umezawa, K. Ogawa, Application of mesenchymal stem cell therapy and inner ear regeneration for hearing loss: a review, Int. J. Mol. Sci. 21 (16) (2020), https://doi.org/10.3390/ijms21165764.

[4] W.J. McLean, D.T. McLean, R.A. Eatock, A.S. Edge, Distinct capacity for differentiation to inner ear cell types by progenitor cells of the cochlea and vestibular organs, Development 143 (23) (2016) 4381–4393, https://doi.org/10.1242/dev.139840.

[5] D. You, L. Guo, W. Li, S. Sun, Y. Chen, R. Chai, et al., Characterization of Wnt and notch-responsive Lgr5+ hair cell progenitors in the striolar region of the neonatal mouse utricle, Front. Mol. Neurosci. 11 (2018), https://doi.org/10.3389/fnmol.2018.00137.

[6] M. Xia, J. Ma, M. Wu, L. Guo, Y. Chen, G.-l. Li, et al., Generation of innervated cochlear organoid recapitulates early development of auditory unit, Stem Cell Rep. 18 (1) (2023) 319–336, https://doi.org/10.1016/j.stemcr.2022.11.024.

[7] H. Lang, Y. Xing, L.N. Brown, D.J. Samuvel, C.H. Panganiban, L.T. Havens, et al., Neural stem/progenitor cell properties of glial cells in the adult mouse auditory nerve, Sci. Rep. 5 (2015) 13383, https://doi.org/10.1038/srep13383.

[8] L.L. Sandell, N.E. Butler Tjaden, A.J. Barlow, P.A. Trainor, Cochleovestibular nerve development is integrated with migratory neural crest cells, Dev. Biol. 385 (2) (2014) 200–210, https://doi.org/10.1016/j.ydbio.2013.11.009.

[9] I. Breuskin, M. Bodson, N. Thelen, M. Thiry, L. Borgs, L. Nguyen, et al., Glial but not neuronal development in the cochleo-vestibular ganglion requires Sox10, J. Neurochem. 114 (6) (2010) 1827–1839, https://doi.org/10.1111/j.1471-4159.2010.06897.x.

[10] W. Tang, Y. Zhang, Q. Chang, S. Ahmad, I. Dahlke, H. Yi, et al., Connexin29 is highly expressed in cochlear Schwann cells, and it is required for the normal development and function of the auditory nerve of mice, J. Neurosci. 26 (7) (2006) 1991–1999, https://doi.org/10.1523/JNEUROSCI.5055-05.2006.

[11] L.N. Pettingill, R.L. Minter, R.K. Shepherd, Schwann cells genetically modified to express neurotrophins promote spiral ganglion neuron survival in vitro, Neuroscience 152 (3) (2008) 821–828, https://doi.org/10.1016/j.neuroscience.2007.11.057.

[12] M.R. Hansen, U. Vijapurkar, J.G. Koland, S.H. Green, Reciprocal signaling between spiral ganglion neurons and Schwann cells involves neuregulin and neurotrophins, Hear. Res. 161 (1–2) (2001) 87–98, https://doi.org/10.1016/s0378-5955(01)00360-4.

[13] G. Wan, G. Corfas, Transient auditory nerve demyelination as a new mechanism for hidden hearing loss, Nat. Commun. 8 (2017) 14487, https://doi.org/10.1038/ncomms14487.

[14] H. Rask-Andersen, M. Bostrom, B. Gerdin, A. Kinnefors, G. Nyberg, T. Engstrand, et al., Regeneration of human auditory nerve. In vitro/in video demonstration of neural progenitor cells in adult human and Guinea pig spiral ganglion, Hear. Res. 203 (1–2) (2005) 180–191, https://doi.org/10.1016/j.heares.2004.12.005.

[15] Z. Chen, Y. Huang, C. Yu, Q. Liu, C. Qiu, G. Wan, Cochlear Sox2(+) glial cells are potent progenitors for spiral ganglion neuron reprogramming induced by small molecules, Front. Cell Dev. Biol. 9 (2021) 728352, https://doi.org/10.3389/fcell.2021.728352.

[16] K. Nishimura, T. Nakagawa, T. Sakamoto, J. Ito, Fates of murine pluripotent stem cell-derived neural progenitors following transplantation into mouse cochleae, Cell Transplant. 21 (4) (2012) 763–771, https://doi.org/10.3727/096368911X623907.

[17] M. Wegner, From head to toes: the multiple facets of Sox proteins, Nucleic Acids Res. 27 (6) (1999) 1409–1420, https://doi.org/10.1093/nar/27.6.1409.

[18] I. Breuskin, M. Bodson, N. Thelen, M. Thiry, L. Borgs, L. Nguyen, et al., Sox10 promotes the survival of cochlear progenitors during the establishment of the organ of Corti, Dev. Biol. 335 (2) (2009) 327–339, https://doi.org/10.1016/j.ydbio.2009.09.007.

[19] L. Freyer, V. Aggarwal, B.E. Morrow, Dual embryonic origin of the mammalian otic vesicle forming the inner ear, Development 138 (24) (2011) 5403–5414, https://doi.org/10.1242/dev.069849.

[20] M. Xia, Y. Chen, Y. He, H. Li, W. Li, Activation of the RhoA-YAP-beta-catenin signaling axis promotes the expansion of inner ear progenitor cells in 3D culture, Stem Cell. 38 (7) (2020) 860–874, https://doi.org/10.1002/stem.3175.

[21] H.T. Chang, R.A. Heuer, A.M. Oleksijew, K.S. Coots, C.B. Roque, K.T. Nella, et al., An engineered three-dimensional stem cell niche in the inner ear by applying a nanofibrillar cellulose hydrogel with a sustained-release neurotrophic factor delivery system, Acta Biomater. 108 (2020) 111–127, https://doi.org/10.1016/j.actbio.2020.03.007.

[22] K.R. Koehler, E. Hashino, 3D mouse embryonic stem cell culture for generating inner ear organoids, Nat. Protoc. 9 (6) (2014) 1229–1244, https://doi.org/10.1038/nprot.2014.100.

[23] L. Shi, G. Hong, C. Chen, X. Li, H. Zhang, R. Chai, et al., Growth of spiral ganglion neurons induced by graphene oxide/oxidized bacterial cellulose composite hydrogel, Carbohydr. Polym. (2023) 311, https://doi.org/10.1016/j.carbpol.2023.120749.

[24] M. Ishikawa, H. Ohnishi, D. Skerleva, T. Sakamoto, N. Yamamoto, A. Hotta, et al., Transplantation of neurons derived from human iPS cells cultured on collagen matrix into Guinea-pig cochleae, J. Tissue Eng. Regen. Med. 11 (6) (2017) 1766–1778, https://doi.org/10.1002/term.2072.

[25] I. Arnaoutova, J. George, H.K. Kleinman, G. Benton, Basement membrane matrix (BME) has multiple uses with stem cells, Stem Cell Rev. Rep. 8 (1) (2012) 163–169, https://doi.org/10.1007/s12015-011-9278-y.

[26] G. Sun, W. Liu, Z. Fan, D. Zhang, Y. Han, L. Xu, et al., The three-dimensional culture system with matrigel and neurotrophic factors preserves the structure and function of spiral ganglion neuron in vitro, Neural Plast. 2016 (2016) 4280407, https://doi.org/10.1155/2016/4280407.

[27] M. Alessandri, G. Lizzo, C. Gualandi, C. Mangano, A. Giuliani, M.L. Focarete, et al., Influence of biological matrix and artificial electrospun scaffolds on proliferation, differentiation and trophic factor synthesis of rat embryonic stem cells, Matrix Biol. 33 (2014) 68–76, https://doi.org/10.1016/j.matbio.2013.08.001.
[28] B.J. Kang, H.H. Ryu, S.S. Park, Y. Kim, H.M. Woo, W.H. Kim, et al., Effect of matrigel on the osteogenic potential of canine adipose tissue-derived mesenchymal stem cells, J. Vet. Med. Sci. 74 (7) (2012) 827–836, https://doi.org/10.1292/jvms.11-0484.
[29] A. Musah-Eroje, S. Watson, A novel 3D in vitro model of glioblastoma reveals resistance to temozolomide which was potentiated by hypoxia, J. Neuro Oncol. 142 (2) (2019) 231–240, https://doi.org/10.1007/s11060-019-03107-0.
[30] T.K. Matsui, M. Matsubayashi, Y.M. Sakaguchi, R.K. Hayashi, C. Zheng, K. Sugie, et al., Six-month cultured cerebral organoids from human ES cells contain matured neural cells, Neurosci. Lett. 670 (2018) 75–82, https://doi.org/10.1016/j.neulet.2018.01.040.
[31] R. Patel, S. Page, A.J. Al-Ahmad, Isogenic blood-brain barrier models based on patient-derived stem cells display inter-individual differences in cell maturation and functionality, J. Neurochem. 142 (1) (2017) 74–88, https://doi.org/10.1111/jnc.14040.
[32] C. Bu, L. Xu, Y. Han, M. Wang, X. Wang, W. Liu, et al., c-Myb protects cochlear hair cells from cisplatin-induced damage via the PI3K/Akt signaling pathway, Cell Death Discov. 8 (1) (2022), https://doi.org/10.1038/s41420-022-00879-9.
[33] Z. Cao, Q. Yang, H. Yin, Q. Qi, H. Li, G. Sun, et al., Peroxynitrite induces apoptosis of mouse cochlear hair cells via a Caspase-independent pathway in vitro, Apoptosis 22 (11) (2017) 1419–1430, https://doi.org/10.1007/s10495-017-1417-8.
[34] T. Wakaoka, T. Motohashi, H. Hayashi, B. Kuze, M. Aoki, K. Mizuta, et al., Tracing Sox10-expressing cells elucidates the dynamic development of the mouse inner ear, Hear. Res. 302 (2013) 17–25, https://doi.org/10.1016/j.heares.2013.05.003.
[35] X.-J. Li, A. Doetzlhofer, LIN28B/let-7 control the ability of neonatal murine auditory supporting cells to generate hair cells through mTOR signaling, Proc. Natl. Acad. Sci. USA 117 (36) (2020) 22225–22236, https://doi.org/10.1073/pnas.2000417117.
[36] I. Smeti, I. Watabe, E. Savary, A. Fontbonne, A. Zine, HMGA2, the architectural transcription factor high mobility group, is expressed in the developing and mature mouse cochlea, PLoS One 9 (2) (2014) e88757, https://doi.org/10.1371/journal.pone.0088757.
[37] A.J. Matsuoka, Z.D. Morrissey, C. Zhang, K. Homma, A. Belmadani, C.A. Miller, et al., Directed differentiation of human embryonic stem cells toward placode-derived spiral ganglion-like sensory neurons, Stem Cells Transl. Med. 6 (3) (2017) 923–936, https://doi.org/10.1002/sctm.16-0032.
[38] A. Kimura, T. Matsuda, A. Sakai, N. Murao, K. Nakashima, HMGB2 expression is associated with transition from a quiescent to an activated state of adult neural stem cells, Dev. Dynam. 247 (1) (2017) 229–238, https://doi.org/10.1002/dvdy.24559.
[39] A.C. Kokotos, C.B. Harper, J.R.K. Marland, K.J. Smillie, M.A. Cousin, S.L. Gordon, Synaptophysin sustains presynaptic performance by preserving vesicular synaptobrevin-II levels, J. Neurochem. 151 (1) (2019) 28–37, https://doi.org/10.1111/jnc.14797.
[40] C.A. Buchman, R.H. Gifford, D.S. Haynes, T. Lenarz, G. O'Donoghue, O. Adunka, et al., Unilateral cochlear implants for severe, profound, or moderate sloping to profound bilateral sensorineural hearing loss: a systematic review and consensus statements, JAMA Otolaryngol Head Neck Surg. 146 (10) (2020) 942–953, https://doi.org/10.1001/jamaoto.2020.0998.
[41] X. Li, A. Aleardi, J. Wang, Y. Zhou, R. Andrade, Z. Hu, Differentiation of spiral ganglion-derived neural stem cells into functional synaptogenetic neurons, Stem Cell. Dev. 25 (10) (2016) 803–813, https://doi.org/10.1089/scd.2015.0345.
[42] M. Diensthuber, V. Zecha, J. Wagenblast, S. Arnhold, A.S.B. Edge, T. Stöver, Spiral ganglion stem cells can Be propagated and differentiated into neurons and glia, BioResearch Open Access 3 (3) (2014) 88–97, https://doi.org/10.1089/biores.2014.0016.
[43] X. Liu, S. Shi, Q. Feng, A. Bachhuka, W. He, Q. Huang, et al., Surface chemical gradient affects the differentiation of human adipose-derived stem cells via ERK1/2 signaling pathway, ACS Appl. Mater. Interfaces 7 (33) (2015) 18473–18482, https://doi.org/10.1021/acsami.5b04635.
[44] B.M. Baker, C.S. Chen, Deconstructing the third dimension: how 3D culture microenvironments alter cellular cues, J. Cell Sci. 125 (Pt 13) (2012) 3015–3024, https://doi.org/10.1242/jcs.079509.
[45] N. Wang, J.D. Tytell, D.E. Ingber, Mechanotransduction at a distance: mechanically coupling the extracellular matrix with the nucleus, Nat. Rev. Mol. Cell Biol. 10 (1) (2009) 75–82, https://doi.org/10.1038/nrm2594.
[46] H.M. Langevin, N.A. Bouffard, G.J. Badger, J.C. Iatridis, A.K. Howe, Dynamic fibroblast cytoskeletal response to subcutaneous tissue stretch ex vivo and in vivo, Am. J. Physiol. Cell Physiol. 288 (3) (2005) C747–C756, https://doi.org/10.1152/ajpcell.00420.2004.
[47] A.D. Doyle, N. Carvajal, A. Jin, K. Matsumoto, K.M. Yamada, Local 3D matrix microenvironment regulates cell migration through spatiotemporal dynamics of contractility-dependent adhesions, Nat. Commun. 6 (2015) 8720, https://doi.org/10.1038/ncomms9720.
[48] R. Martinez-Monedero, C.E. Corrales, M.P. Cuajungco, S. Heller, A.S. Edge, Reinnervation of hair cells by auditory neurons after selective removal of spiral ganglion neurons, J. Neurobiol. 66 (4) (2006) 319–331, https://doi.org/10.1002/neu.20232.
[49] S.J. Kim, J.Y. Lim, J.N. Lee, S.K. Choe, Y.I. Kim, S.R. Song, et al., Activation of beta-catenin by inhibitors of glycogen synthase kinase-3 ameliorates cisplatin-induced cytotoxicity and pro-inflammatory cytokine expression in HEI-OC1 cells, Toxicology 320 (2014) 74–82, https://doi.org/10.1016/j.tox.2014.01.013.
[50] J.A. Burdick, G. Vunjak-Novakovic, Engineered microenvironments for controlled stem cell differentiation, Tissue Eng. 15 (2) (2009) 205–219, https://doi.org/10.1089/ten.tea.2008.0131.
[51] G. Miao, Y. Zhao, Y. Li, J. Xu, H. Gong, R. Qi, et al., Basement membrane extract preserves islet viability and activity in vitro by up-regulating alpha3 integrin and its signal, Pancreas 42 (6) (2013) 971–976, https://doi.org/10.1097/MPA.0b013e318287cfe0.
[52] S. Yui, T. Nakamura, T. Sato, Y. Nemoto, T. Mizutani, X. Zheng, et al., Functional engraftment of colon epithelium expanded in vitro from a single adult Lgr5(+) stem cell, Nat. Med. 18 (4) (2012) 618–623, https://doi.org/10.1038/nm.2695.
[53] H. Yin, Y. Sun, B. Ya, Y. Guo, H. Zhao, L. Zhang, et al., Apelin-13 protects against cisplatin-induced ototoxicity by inhibiting apoptosis and regulating STAT1 and STAT3, Arch. Toxicol. 97 (9) (2023) 2477–2493, https://doi.org/10.1007/s00204-023-03544-x.
[54] W. Liu, X. Xu, Z. Fan, G. Sun, Y. Han, D. Zhang, et al., Wnt signaling activates TP53-induced glycolysis and apoptosis regulator and protects against cisplatin-induced spiral ganglion neuron damage in the mouse cochlea, Antioxidants Redox Signal. 30 (11) (2019) 1389–1410, https://doi.org/10.1089/ars.2017.7288.
[55] W. Liu, L. Xu, X. Wang, D. Zhang, G. Sun, M. Wang, et al., PRDX1 activates autophagy via the PTEN-AKT signaling pathway to protect against cisplatin-induced spiral ganglion neuron damage, Autophagy 17 (12) (2021) 4159–4181, https://doi.org/10.1080/15548627.2021.1905466.
[56] Z. Liu, M. Tang, J. Zhao, R. Chai, J. Kang, Looking into the future: toward advanced 3D biomaterials for stem-cell-based regenerative medicine, Adv. Mater. 30 (17) (2018) e1705388, https://doi.org/10.1002/adma.201705388.
[57] D. Guseva, I. Jakovcevski, A. Irintchev, I. Leshchyns'ka, V. Sytnyk, E. Ponimaskin, et al., Cell adhesion molecule close homolog of L1 (CHL1) guides the regrowth of regenerating motor axons and regulates synaptic coverage of motor neurons, Front. Mol. Neurosci. 11 (2018), https://doi.org/10.3389/fnmol.2018.00174.
[58] S. Samanta, L. Ylä-Outinen, V.K. Rangasami, S. Narkilahti, O.P. Oommen, Bidirectional cell-matrix interaction dictates neuronal network formation in a brain-mimetic 3D scaffold, Acta Biomater. 140 (2022) 314–323, https://doi.org/10.1016/j.actbio.2021.12.010.
[59] S.J. Baker, R. Sumerson, C.D. Reddy, A.S. Berrebi, D.C. Flynn, E.P. Reddy, Characterization of an alternatively spliced AATYK mRNA: expression pattern of AATYK in the brain and neuronal cells, Oncogene 20 (9) (2001) 1015–1021, https://doi.org/10.1038/sj.onc.1204209.
[60] W. Zhang, X. Zhu, Y. Liu, M. Chen, S. Yan, X. Mao, et al., Nur77 was essential for neurite outgrowth and involved in schwann cell differentiation after sciatic nerve injury, J. Mol. Neurosci. 57 (1) (2015) 38–47, https://doi.org/10.1007/s12031-015-0575-9.
[61] H.G. Ryu, J.-Y. Seo, Y. Jung, S.W. Kim, E. Kim, S.K. Jang, et al., Upf1 regulates neurite outgrowth and branching by transcriptional and post-transcriptional modulation of Arc, J. Cell Sci. (2018), https://doi.org/10.1242/jcs.224055.
[62] N. Watanabe, M. Itakaoka, Y. Seki, T. Morimoto, K. Homma, Y. Miyamoto, et al., Dystonia-4 (DYT4)-associated TUBB4A mutants exhibit disorganized microtubule networks and inhibit neuronal process growth, Biochem. Biophys. Res. Commun. 495 (1) (2018) 346–352, https://doi.org/10.1016/j.bbrc.2017.11.038.
[63] P.A.R. Ekström, U. Mayer, A. Panjwani, D. Pountney, J. Pizzey, D.A. Tonge, Involvement of α7β1 integrin in the conditioning-lesion effect on sensory axon regeneration, Mol. Cell. Neurosci. 22 (3) (2003) 383–395, https://doi.org/10.1016/s1044-7431(02)00034-9.
[64] B.-R. She, G.-G. Liou, S. Lin-Chao, Association of the growth-arrest-specific protein Gas7 with F-actin induces reorganization of microfilaments and promotes membrane outgrowth, Exp. Cell Res. 273 (1) (2002) 34–44, https://doi.org/10.1006/excr.2001.5435.
[65] L. Annunziato, D.M. O'Halloran, Simulation model of CA1 pyramidal neurons reveal opposing roles for the Na+/Ca2+ exchange current and Ca2+-activated K+ current during spike-timing dependent synaptic plasticity, PLoS One 15 (3) (2020), https://doi.org/10.1371/journal.pone.0230327.
[66] P. Rebellato, D. Kaczynska, S. Kanatani, I.A. Rayyes, S. Zhang, C. Villaescusa, et al., The T-type Ca2+ channel Cav3.2 regulates differentiation of neural progenitor cells during cortical development via caspase-3, Neuroscience 402 (2019) 78–89, https://doi.org/10.1016/j.neuroscience.2019.01.015.
[67] E. Takahashi, K. Sagane, T. Oki, K. Yamazaki, T. Nagasu, J. Kuromitsu, Deficits in spatial learning and motor coordination in ADAM11-deficient mice, BMC Neurosci. 7 (1) (2006), https://doi.org/10.1186/1471-2202-7-19.
[68] J.B. Ding, W.-J. Oh, B.L. Sabatini, C. Gu, Semaphorin 3E–Plexin-D1 signaling controls pathway-specific synapse formation in the striatum, Nat. Neurosci. 15 (2) (2011) 215–223, https://doi.org/10.1038/nn.3003.
[69] H. Guo, Y. Jiang, Z. Gu, L. Ren, C. Zhu, S. Yu, et al., ZFP36 protects against oxygen-glucose deprivation/reoxygenation-induced mitochondrial fragmentation and neuronal apoptosis through inhibiting NOX4-DRP1 pathway, Brain Res. Bull. 179 (2022) 57–67, https://doi.org/10.1016/j.brainresbull.2021.12.003.

[70] M.J. Pérez, T.R. Carden, P.A. dos Santos Claro, S. Silberstein, P.M. Páez, V.T. Cheli, et al., Transferrin enhances neuronal differentiation, ASN Neuro (2023) 15, https://doi.org/10.1177/17590914231170703.
[71] S. Leppä, M. Eriksson, R. Saffrich, W. Ansorge, D. Bohmann, Complex functions of AP-1 transcription factors in differentiation and survival of PC12 cells, Mol. Cell Biol. 21 (13) (2023) 4369–4378, https://doi.org/10.1128/mcb.21.13.4369-4378.2001.
[72] K.-H. Schlingensiepen, F. Wollnik, M. Kunst, R. Schlingensiepen, T. Herdegen, W. Brysch, The role of Jun transcription factor expression and phosphorylation in neuronal differentiation, neuronal cell death, and plastic adaptationsin vivo, Cell. Mol. Neurobiol. 14 (5) (1994) 487–505, https://doi.org/10.1007/bf02088833.
[73] D. Vaudry, P.J.S. Stork, P. Lazarovici, L.E. Eiden, Signaling pathways for PC12 cell differentiation: making the right connections, Science 296 (5573) (2002) 1648–1649, https://doi.org/10.1126/science.1071552.
[74] L. Ou, W. Li, Y. Zhang, W. Wang, J. Liu, H. Sorg, et al., Intracardiac injection of matrigel induces stem cell recruitment and improves cardiac functions in a rat myocardial infarction model, J. Cell Mol. Med. 15 (6) (2011) 1310–1318, https://doi.org/10.1111/j.1582-4934.2010.01086.x.